

AD-762 812

BORON NITRIDE DIFFUSION FOR LSI
PROCESSING

J. Stach, et al

Pennsylvania State University

Prepared for:

Army Electronics Command

March 1973

DISTRIBUTED BY:

NTIS

National Technical Information Service
U. S. DEPARTMENT OF COMMERCE
5285 Port Royal Road, Springfield Va. 22151

AD



AD 762812

Research and Development Technical Report

ECOM-0200-F

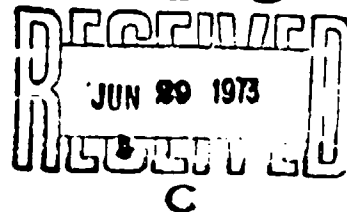
C299

BORON NITRIDE DIFFUSION FOR LSI PROCESSING FINAL REPORT

by

J. STACH - D. RUPPRECHT - A. TURLEY

D D C



MARCH 1973

Distribution Statement

This document has been approved
for public release and sale; its
distribution is unlimited.

Reproduced by
NATIONAL TECHNICAL
INFORMATION SERVICE
US Department of Commerce
Springfield VA 22151

ECOM

UNITED STATES ARMY ELECTRONICS COMMAND - FORT MONMOUTH, N.J.

CONTRACT DAAB07-71-C-0299

THE PENNSYLVANIA STATE UNIVERSITY

UNIVERSITY PARK, PENNSYLVANIA 16802

Disclaimers

The findings in this report are not to be construed as an official Department of the Army position, unless so designated by other authorized documents.

The citation of trade names and names of manufacturers in this report is not to be construed as official Government indorsement or approval of commercial products or services referenced herein.

Disposition

Destroy this report when it is no longer needed. Do not return it to the originator.

ACCOMPLISHED BY	
NTSB	✓
DOC	
UNANNOUNCED	
JUSTIFICATION	
BY	
DISTRIBUTION/AVAILABILITY CODES	
Dist.	AVAIL. and/or SPECIAL

TABLE OF CONTENTS

	Page
Abstract	1
List of Figures	ii-iii
List of Tables	iv
Introduction	1-2
BN Surface Kinetics	2-18
BN Source Impurities	16
Furnace System Optimization	16-36
Characterization of BN Diffusion Behavior . .	36-47
BN Source Composition	48
N Type Source Evaluation	56-57
References	58-59

ABSTRACT

The report describes the properties and behavior of boron nitride diffusion wafers for use in LSI processing. The results of the investigations conducted include the determination of proper handling procedures, B_2O_3 growth and volatilization kinetics, furnace parameters, and reliability and reproducibility.

LIST OF FIGURES

- Figure 1 - Linear Plot of % Weight Increase as a Function of Gas Ambient
- Figure 2 - Log-Log Plot of % Weight Increase as a Function of Gas Ambient
- Figure 3 - Spectrograph of Oxidized ABN
- Figure 4 - TGA of Etched and Unetched MBN
- Figure 5 - MOS C-V Plot of Control Wafer
- Figure 5a - MOS C-V Plot of Oxide Exposed to MBN
- Figure 6 - Stacking Arrangement of BN and Silicon Wafers
- Figure 7 - Sheet Resistance Versus Flow Rate
- Figure 8 - Sheet Resistance Versus Time and Ambient
- Figure 9 - Positional Relationship Between Silicon and BN for Sheet Resistance Versus Spacing
- Figure 10 - Sheet Resistance Versus Spacing
- Figure 11 - Helium Ambient Impurity Profile
- Figure 12 - Argon Ambient Impurity Profile
- Figure 13 - Sheet Resistance Versus Flow Rate for 1100°C Diffusions
- Figure 14 - Sheet Resistance Versus Flow Rate for 1200°C Diffusions
- Figure 15 - Sheet Resistance Versus Spacing with Gas Ambient as a Parameter
- Figure 16 - Sheet Resistance Versus Time, Temperature and Spacing
- Figure 17 - Sheet Resistance Versus Time from 1000°C to 1200°C in Various Ambients
- Figure 18 - Diffused Impurity Profile Showing the Effects of Inert Gas Ambient
- Figure 19 - Sheet Resistance Versus Run Number

LIST OF FIGURES (cont.)

- Figure 20 - Reproducibility of Sheet Resistance from Run to Run with Gas Ambient and Flow Rate as Parameters
- Figure 21 - % Sheet Resistance Variation Across Silicon Wafer
- Figure 22 - Across Wafer Uniformity at 1100°C for Diffusions Done in a Nitrogen Ambient
- Figure 23 - Across Wafer Uniformity of Sheet Resistance for Diffusion at 1100°C in an Argon Ambient
- Figure 24 - Percentage Variation of Sheet Resistance Across the Wafer Area for Diffusions at 1100°C in a Helium Ambient
- Figure 25 - Log-Log Plot of % Weight Increase as a Function of Time, Ambient and BN Wafer Density
- Figure 26 - Log-Log Plot of % Weight Increase as a Function of Time, Ambient and B_2O_3 Binder Concentration
- Figure 27 - % Sheet Resistance Variation Across Silicon Wafer for 93% BN and 80% BN/20% SiO_2
- Figure 28 - Sheet Resistance Distribution
- Figure 29 - Sheet Resistance, Junction Depth Versus Time - 1100°C
- Figure 30 - Oxide Formation, PSG Penetration Versus Time, 1100°C

LIST OF TABLES

- Table 1 - Physical Properties of Boron Nitride
- Table 2 - Summary of Cleaning Chemicals ABN
- Table 3 - Summary of Cleaning Chemicals MBN
- Table 4 - Cleaning and Handling Procedures for ABN
- Table 5 - Cleaning and Handling Procedures for MBN
- Table 6 - Ellipsometric Data for Various Spacings
During Diffusion

INTRODUCTION

With the advent of LSI (large scale integrated circuits), it became apparent that the commonly used carrier gas diffusion systems which employ liquids and gases as sources did not afford the degree of control over large areas which is necessary in LSI processing. A planar wafer diffusion source such as boron nitride offers an attractive alternative based on mass transport by diffusion rather than the more common carrier gas systems. The goal of this research program was to characterize the BN planar wafer system in the interest of optimizing its implementation in LSI processing. The specific results of this program are (1) determination of proper handling techniques for BN wafers, (2) determination of the effects of system parameters such as gas flow rates, gas ambient composition, and system geometry on sheet resistance of diffused layers and doping profiles, (3) determination of the reproducibility and uniformity of sheet resistance of diffused layers and, (4) determination of the feasibility of an N type planar wafer source.

The study shows that BN wafers are well suited as diffusion sources for silicon planar technology and offer some definite advantages such as long source lifetime and minimum safety requirements due to its non toxic nature. In the text of the report the designations ABN and MBN are

used to identify two basic types of boron nitride that were investigated. The physical properties of these materials are shown on Table 1.

BN SURFACE KINETICS

In order to establish proper handling procedures for ABN wafers it was necessary to study the effects of various acids and solvents on BN. The selection of solvents and acids used was based on the cleaning procedures successfully employed with silicon (1), and known etchants of ABN (2). Table 2 summarizes the effects of the various cleaning chemicals. The important aspects of this study are:

- (a) The solubility of ABN's B_2O_3 binder in alcohols (3) limits the post trichlorethylene rinse to acetone;
- (b) The solubility of ABN's B_2O_3 binder in strong acids (3), prevents the use of acids for metallic ion leaching; and
- (c) None of the cleaning procedures employed interfered with the ABN's sourcing ability but those procedures utilizing methanol or nitric acid seriously degrade the ABN wafer's physical strength by attacking the

Table 1 - Physical Properties of Boron Nitride

PHYSICAL PROP.	GRADE A	GRADE M	GRADE HP
CHEMICAL COMP.			
BORON	41.50%	17.0%	42.0%
NITROGEN	52.00	23.0	53.5
OXYGEN	4.0-6.0	<.05	1.5-2.5
BORIC OXIDE	5.0-8.0	<.05	<.10
CARBON	<.05	<.75	<.05
CALCIUM	<.20	<.05	1.50
CHLORIDE	<.10	<.05	.20
OTHER	<.20	<.10	<.20
SILICA	-	60.0	-
DENSITY gm/cm ³	2.08	2.12	1.90
MAXIMUM USE TEMP.			
INERT ATMOSPHERE	>2775 °C	1400 °C	>2775 °C
OXIDIZING ATMOSPHERE	985 °C	1400 °C	1200 °C
WATER ABSORPTION % wt. gain in 168 hrs. @ 25°C, 80%RH	1.1	0.04	0.16

Table 2 - Summary of Cleaning Chemicals ABN

CHEMICAL	COMMENTS
TRICHLOROETHYLENE	VISUAL INSPECTION INDICATED SATISFACTORY REMOVAL OF HUMAN OILS; NO DELETERIOUS EFFECTS NOTED
ACETONE	SATISFACTORY SOLVENT FOR TRICHLOROETHYLENE; NO DELETERIOUS EFFECTS NOTED
METHANOL	SATISFACTORY SOLVENT FOR TRICH. BUT SERIOUS LOSS IN BN WAFER STRENGTH NOTED AFTER BRIEF EXPOSURE
NITRIC ACID	SOLVENT FOR MOST TRANSITION METALS; USE SERIOUSLY DECREASED PHYSICAL STRENGTH OF BN WAFER
HYDROFLUORIC ACID	BN ETCHANT; SOLVENT FOR MOST OXIDES BUT NO DELETERIOUS EFFECTS NOTED

binder and occasional delamination of the wafer was observed after high temperature operation. It was also observed that since B_2O_3 is hygroscopic it is necessary to reverse the water hydration that occurs during de-ionized wafer rinsing by drying at $345^{\circ}C$ for 30 minutes in an N_2 ambient. If this drying procedure is not followed explosion, spalling and/or delamination of the ABN wafer occurs upon insertion into a high temperature furnace. The hydration reversal conditions were arrived at using thermogravimetric analysis (TGA) investigations.

To characterize the surface kinetics of ABN in oxidizing and non-oxidizing ambients TGA experiments were conducted. The studies were conducted on 93% BN, 2.08% B_2O_3 binder concentration, 2.01 gms/cm^3 density. Figure 1 shows a TGA in terms of % weight gained and lost as a function of ambient at $950^{\circ}C$. Figure 2 shows a log-log plot of the TGA data with the slope, m , of the oxidation curve equal to 0.86. The two controlling extremes of oxide growth are also shown. For a surface reaction rate limited process, $m=1$ and for a diffusion rate limited

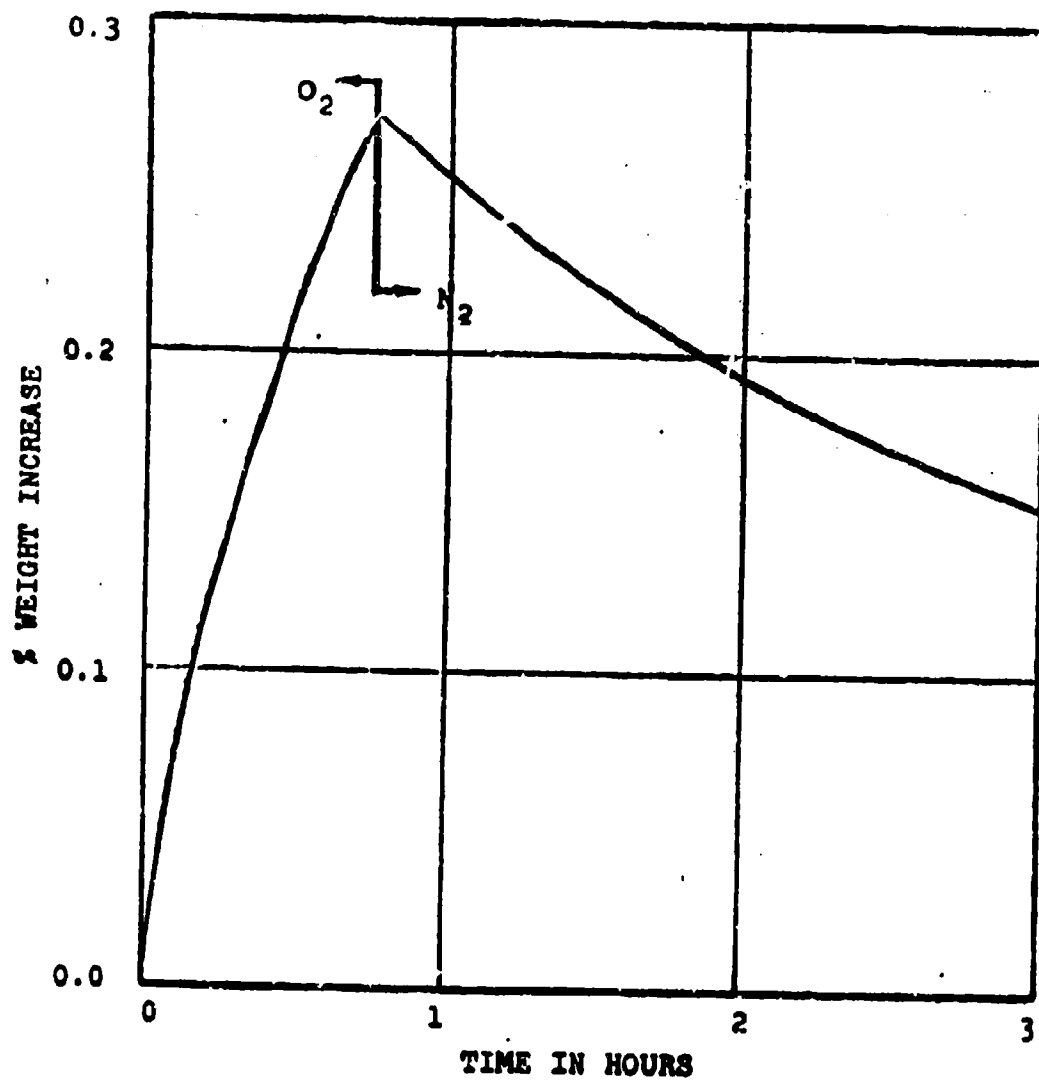


Figure 1 - Linear Plot of % Weight Increase as a Function of Gas Ambient

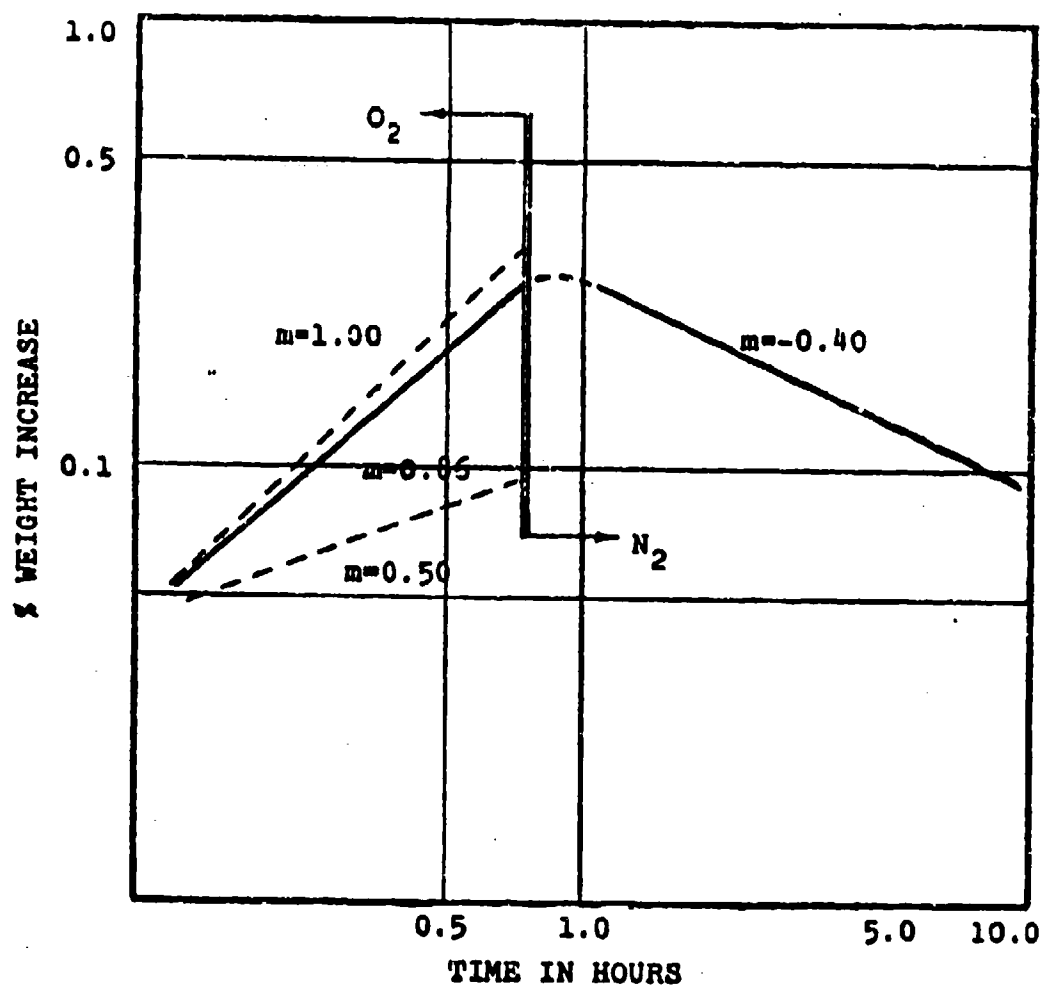


Figure 2 - Log-Log Plot of % Weight Increase as a Function of Gas Ambient

process, $m=0.5$. A comparison of the oxidation rate of ABN in a dry O_2 ambient indicates that a reaction rate limited process dominates the oxidation under these conditions.

The volatilization rate of oxidized ABN in dry N_2 indicates that the wafer will be an effective source for 2000 hours but no attempt was made to verify this experimentally although a continuous run of 146 hours at $950^\circ C$ after a 30 minute oxidation showed no loss in sourcing ability.

To better understand the transport process of a ABN planar wafer diffusion system the dynamic vapor pressure of the volatilizing species was calculated assuming ideal gas law behavior. The dynamic vapor pressure can be calculated using the following equation (4)

$$P_{OxABN} = \frac{(N_{OX\ BN/t})}{N_{TOT/t}} P_{TOT}$$

where

P_{OxABN} - dynamic vapor pressure of oxidized BN

$N_{OxABN/t}$ - moles of oxidized BN lost per unit time

$N_{TOT/t}$ - moles and gas passing by sample per unit time

and

P_{TOT} - total pressure

From the values obtained for actual weight loss data

presented in Figure 2

$$P_{\text{OxABN}} = 4.93 \times 10^{-5} \text{ atm.}$$

When this vapor pressure is compared with that of B_2O_3 obtain by Speiser, et al. (4) and Soulen, et al. (5) for 950°C it is two orders of magnitude greater than the 3×10^{-7} atm. predicted by their experiments. This indicates that the volatilizing species is not totally composed of B_2O_3 .

Studies by Randall and Margrave (6) on vapor equilibrium of the $\text{B}_2\text{O}_3\text{-H}_2\text{O}$ system indicates that a significant increase in vapor pressure of B_2O_3 is observed in the presence of 1% H_2O . Utilizing their results at 1000°C indicates that the presence of 300 PPM H_2O results in a vapor pressure of 5×10^{-5} atm. These suggests that although a hydration removal process is incorporated in the source preparation procedures there exists sufficient residual water vapor in the ABN wafer, possibility in the B_2O_3 binder, to influence its diffusion source properties. Monopole mass spectroscopy was used to tag the diffusing species of a sourcing, ABN wafer. Figure 3 shown the results of the spectrographic studies at 900°C which identifies HBO_2 as the volatilizing species.

Since MBN utilizes silica, SiO_2 , as a binder its handling prior to use as a diffusion source is somewhat different. In addition to the criteria applied to ABN it

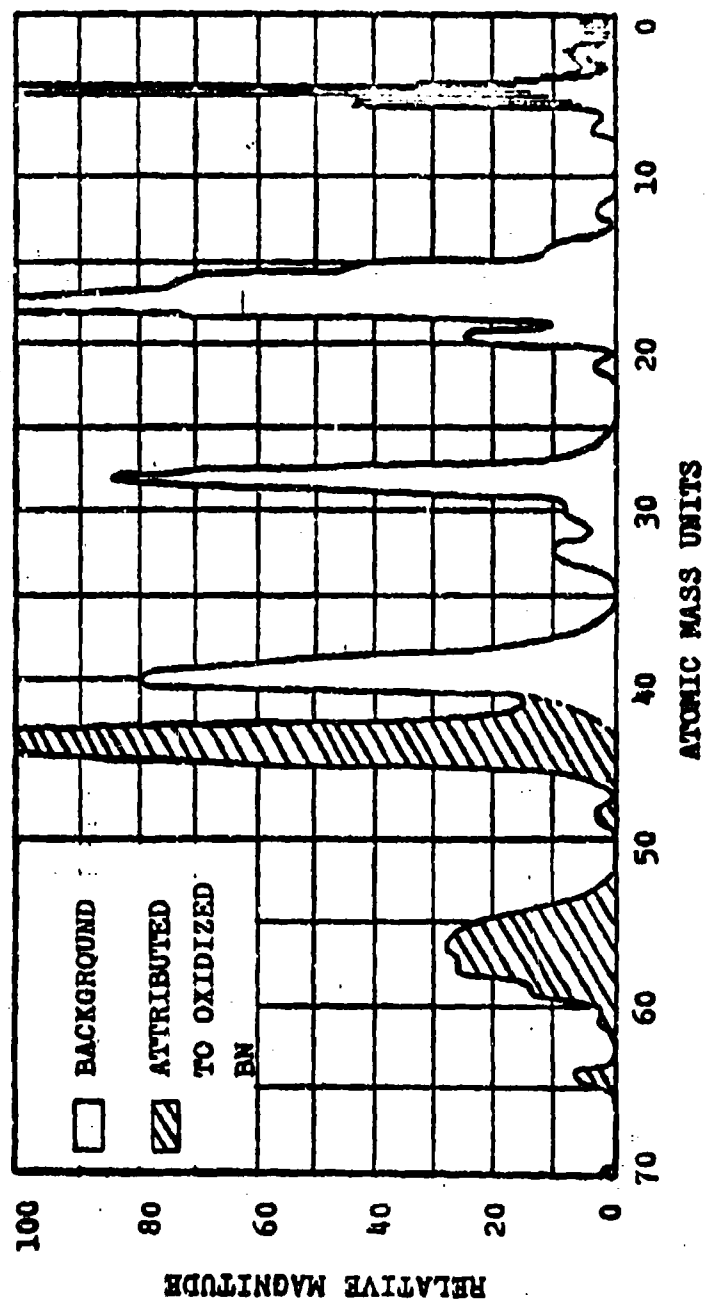
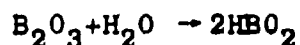
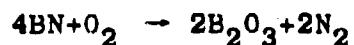


Figure 3 - Spectrograph of Oxidized ABN

was necessary to consider the known etchants of SiO_2 . A summary of the solvents and acids used in the cleaning study is given in Table 3. Because of the high temperature and need for a refluxing apparatus hot phosphoric acid was discarded as a BN etchant in favor of hydrofluoric acid. The most important aspect of this phase of the study was the enhancement of MBN's sourcing ability after HF etching which was subsequently substantiated by TGA studies.

Figure 4 shows a TGA at 1150°C for an HF etched MBN wafer and an unetched wafer. Note the large increase in oxidation and volatilization rates for the etched sample as well as the fact that the % weight change of the etched sample extends into the negative range. This is probably due to the loss of both B_2O_3 and SiO_2 as the wafer volatilizes. As in this case for ABN the dominant volatilizing species is HBO_2 which was determined by thermal vaporization and monopole mass spectroscopy. Thus the sourcing of both ABN and MBN occur via the following proposed reactions:



As a result of the chemical cleaning and the TGA studies the recommended handling procedures for ABN and MBN are given in Tables 4 and 5.

Table 3 - Summary of Cleaning Chemicals MBN

CHEMICAL	COMMENTS
TRICHLORETHYLENE	Visual inspection indicated satisfactory removal of human oils; no deleterious effects were noted.
ACETONE	Satisfactory solvent for trichloroethylene; no deleterious effects were noted.
METHANOL	Satisfactory solvent for trichloroethylene; no deleterious effects were noted.
NITRIC ACID	Solvent for most transition metals; no deleterious effects were noted.
HYDROFLUORIC ACID	BN and SiO_2 etchant, solvent for most oxides; no deleterious effects were noted.

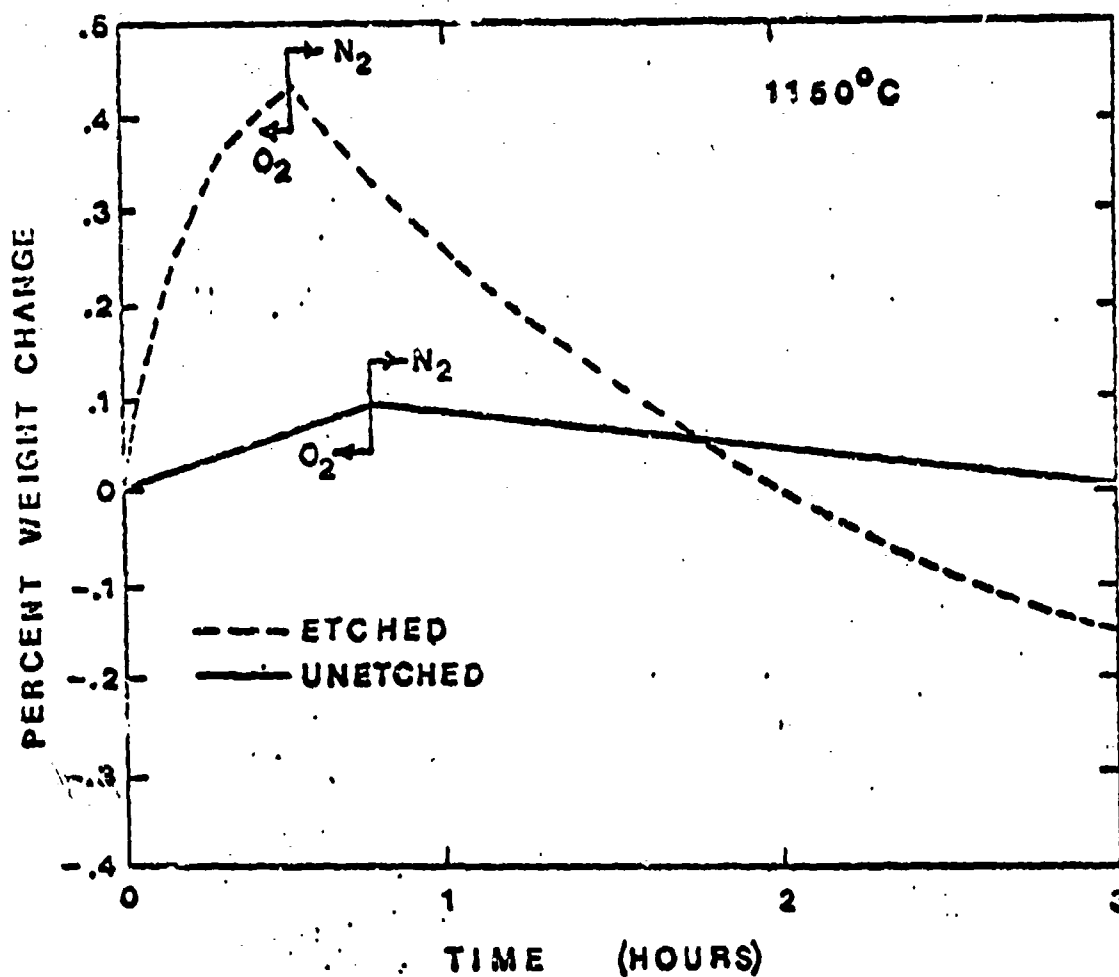


Figure 4 - TGA of Etched and Unetched MBN

Table 4 - Cleaning and Handling Procedures for ABN

CLEANING	<p>a. <u>DEGREASING</u>: Trichlorethylene, 80°C, 3 minutes; Acetone, 40°C, 3 minutes; D I H₂O rinse, 3 minutes</p> <p>b. <u>PREP. OF VIRGIN SURFACE</u>: Conc. HF, 23°C, 1 minute; D I H₂O rinse, until rinse water 10 megohm; dry at 345°C, 30 minutes</p>
OXIDATION	<p>a. <u>TEMPERATURE</u>: At desired deposition temperature</p> <p>b. <u>TIME</u>: 15 minutes</p> <p>c. <u>AMBIENT</u>: 0.5 to 1.0 LPM dry O₂</p>
STABILIZATION	<p>a. <u>TEMPERATURE</u>:</p> <p>b. <u>TIME</u>: 30 minutes</p> <p>c. <u>AMBIENT</u>: 0.5 - 1.0 LPM dry N₂</p>
STORAGE	<p>a. <u>WHEN</u>: When not using material as a source</p> <p>b. <u>WHERE</u>: Vestibule of capped furnace for end of tube or oven at >200°C with N₂</p>
RE-OXIDATION	<p>a. <u>WHEN</u>: As sheet resistance tolerances demand</p> <p>b. <u>HOW</u>: Follow oxidation; no additional cleaning required.</p>

Table 5 - Cleaning and Handling Procedures for MBN

CLEANING	<p><u>DEGREASING</u>: boil in trichlorethylene for 5 minutes, boil in acetone for 5 minutes, rinse in DI water</p> <p><u>LEACHING METALLIC IONS</u>: boil in nitric acid for 10 minutes, rinse in DI water</p> <p><u>ETCHING SURFACE</u>: immerse in room temperature BHF for 30 seconds, cascade rinse in DI water until resistivity > 10 ohm-cm</p> <p><u>DRYING</u>: 345°C in nitrogen at 1 SLPM</p>
OXIDATION	<p><u>TEMPERATURE</u>: above 1000 C as desired</p> <p><u>TIME</u>: 30 Minutes</p> <p><u>AMBIENT</u>: 100% oxygen at 0.5 SLPM</p>
STABILIZATION	<p><u>TEMPERATURE</u>:</p> <p><u>TIME</u>:</p> <p><u>AMBIENT</u>: 100% N₂ @ 0.5</p>
STORAGE	<p><u>WHERE</u>: vestibule capped furnace or far end of tube or over > 200°C in N₂</p> <p><u>AMBIENT</u>: nitrogen at 0.5 SLPM</p>
REOXIDATION	<p><u>WHEN</u>: when sheet resistance increases</p> <p><u>HOW</u>: etch surface and dry, then proceed with normal oxidation procedure</p>

BN SOURCE IMPURITIES

In order to determine the effect of a BN diffusion process on the stability of oxide layers MOS C-V measurements were performed on oxides exposed to BN diffusions. The original oxides were contaminated as indicated by the C-V curves in Figure 5. The oxides were steam grown at 1150°C for five minutes to obtain an oxide thickness of 2000\AA . The oxidized wafers were then exposed on MBN source wafer at 1100°C for thirty minutes. The C-V plots of the MBN exposed, Figure 5a, oxides are not significantly different from the control silicon wafers.

FURNACE SYSTEM OPTIMIZATION

Because a planar wafer system is significantly different from previous diffusion systems it was necessary to characterize the furnace system in order to optimize BN wafer use as dopant sources. In addition to system geometry, gas flow rates, and gas ambients were studied. Previous work covering parallel to gas flow B_2H_6 pre-diffusions (7) and parallel to gas flow drive-in diffusions (8) have indicated that surface concentration and uniformity of sheet resistance are flow rate dependent. Figure 6 shows the typical stacking arrangement for a BN planar wafer diffusion system. This arrangement makes maximum use of furnace space in order to optimize production use of furnaces.

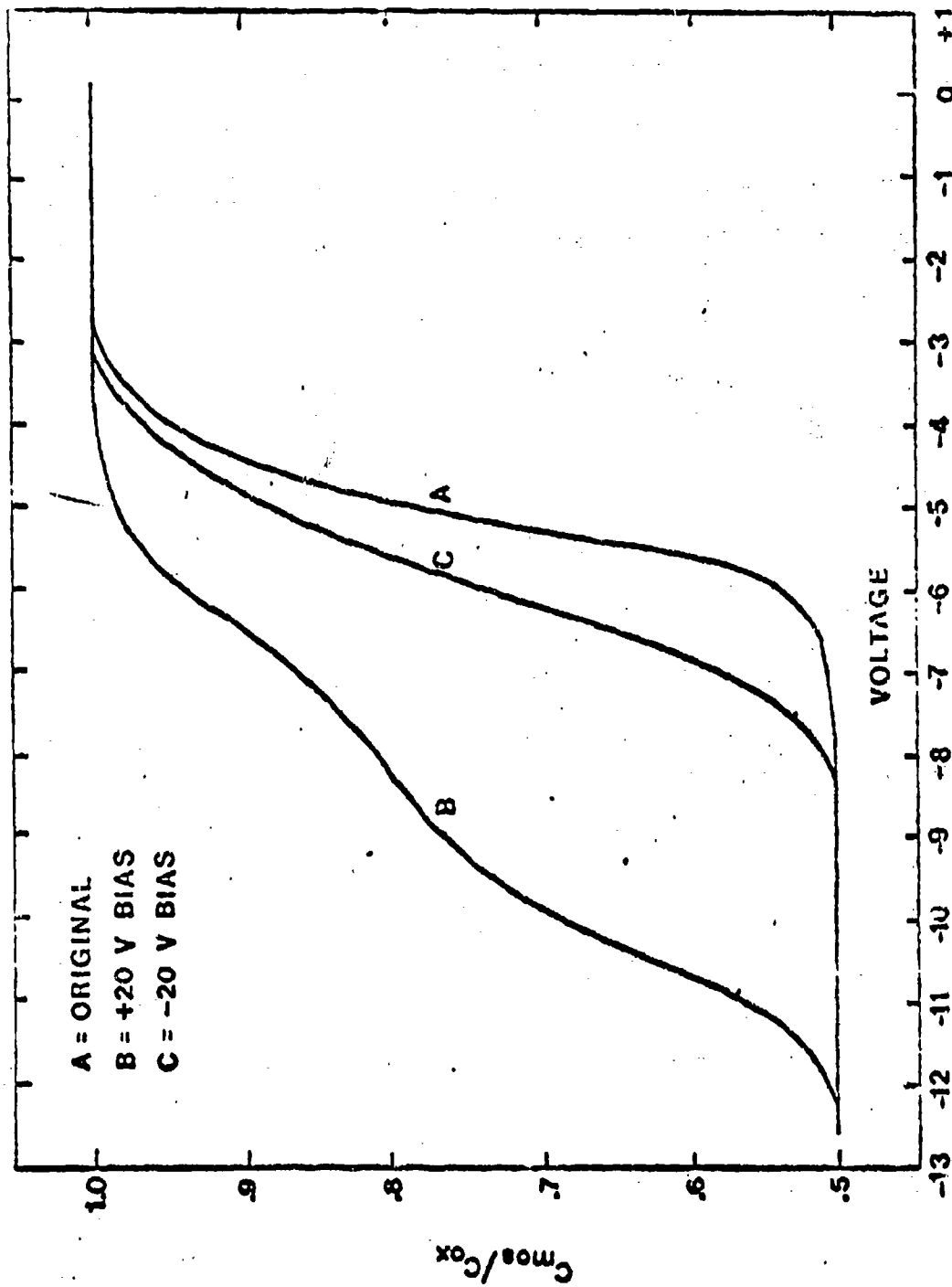


Figure 5 - MOS C-V Plot of Control Wafer

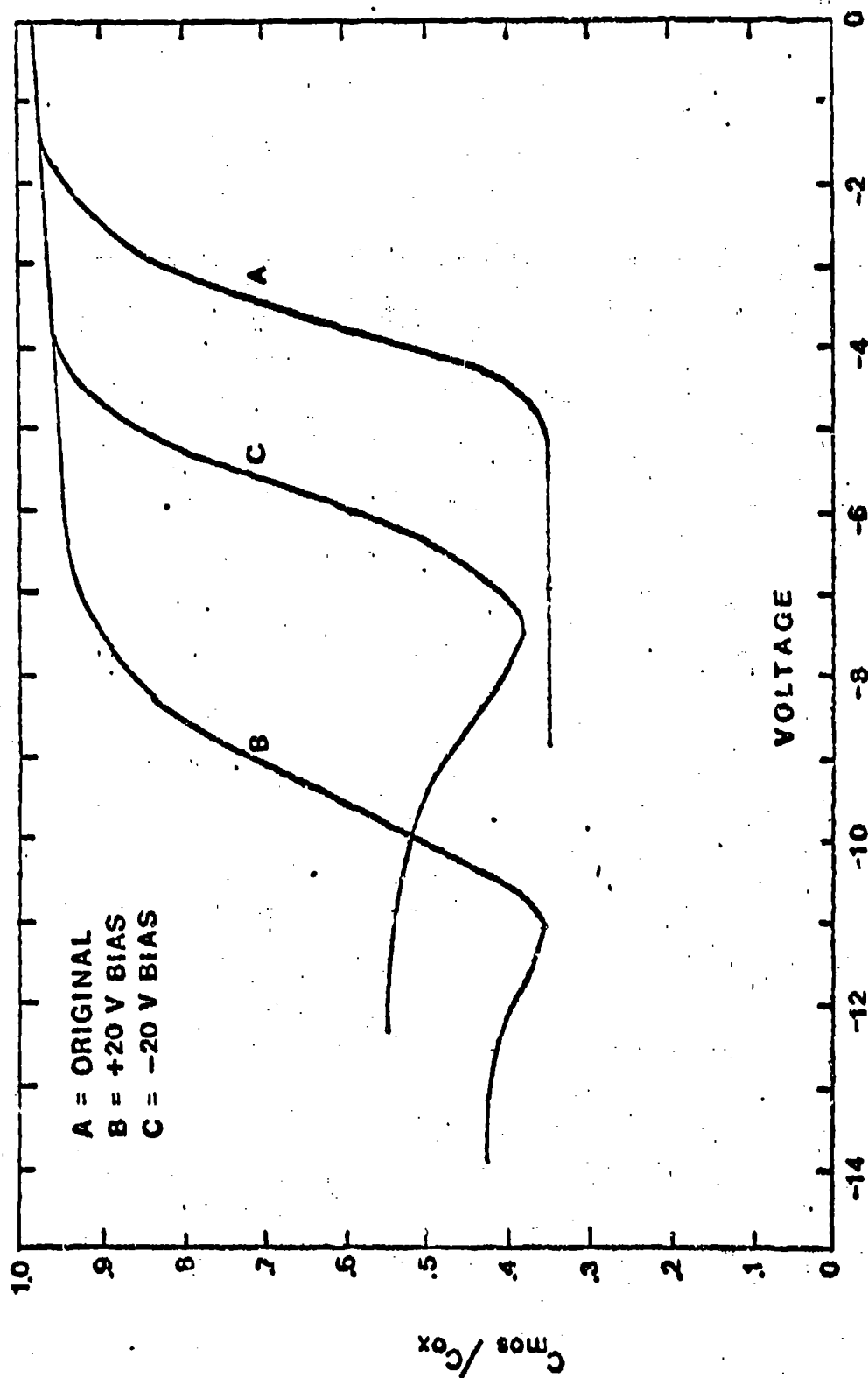


Figure 5a - MOS C-V Plot of Oxide Exposed to MBN

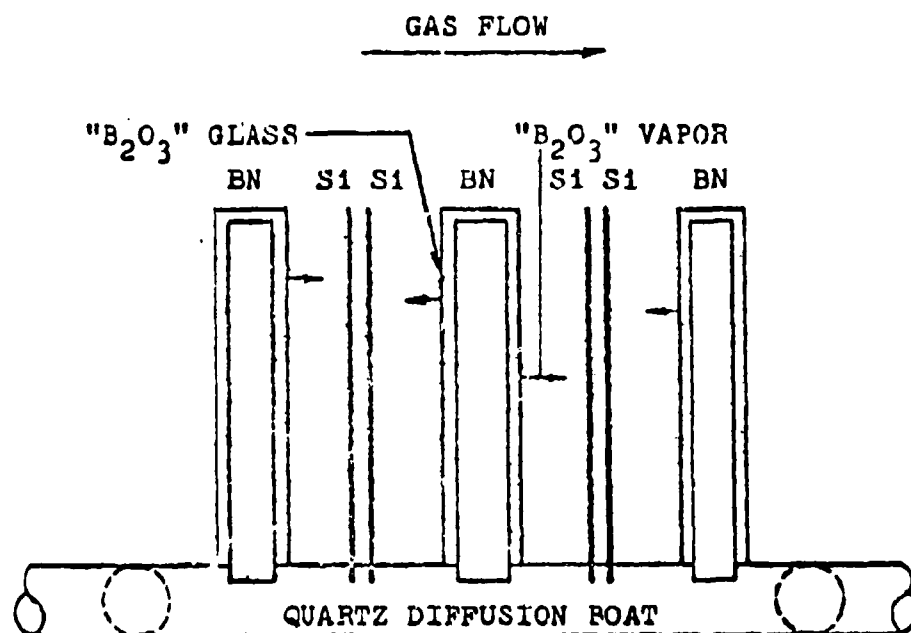


Figure 6 - Stacking Arrangement of BN and Silicon Wafers

The studies made during this phase include flow rate dependence, gas ambient dependence and spacing dependence. These studies were conducted at low temperatures, less than 1000°C using ABN and at high temperatures, greater than 1000°C , using MBN. Although the BN system is not a carrier gas system some flow rate dependence might be expected. To determine the influence of flow rate on uniformity and sheet resistance experiments were conducted at 950°C , for 30 minutes in dry N_2 . Figure 7 shows the flow rate dependence of sheet resistance.

The mechanisms of mass transport for the BN deposition system cannot be easily characterized. A comparison of sheet resistance obtained for 30 minutes, 950°C , N_2 ambient, no gas flow ($\bar{\rho}_s = 50$ ohms per square) and a 30 minute, 950°C , N_2 ambient flowing at 0.45 slpm ($\bar{\rho}_s = 62$ ohms per square) indicates that the system with gas flow cannot be approximated by a stagnant system in which mass transport is by concentration gradient diffusion done. However, the influence of turbulence can be ruled out since the Reynolds number for our system, gas flow through an annular ring, is one and in order to have turbulence the Reynolds number must exceed 2000. Because of this it is appropriate to assume that Fick's Law is applicable as shown below

$$J = -D \frac{dX_A}{dx}$$

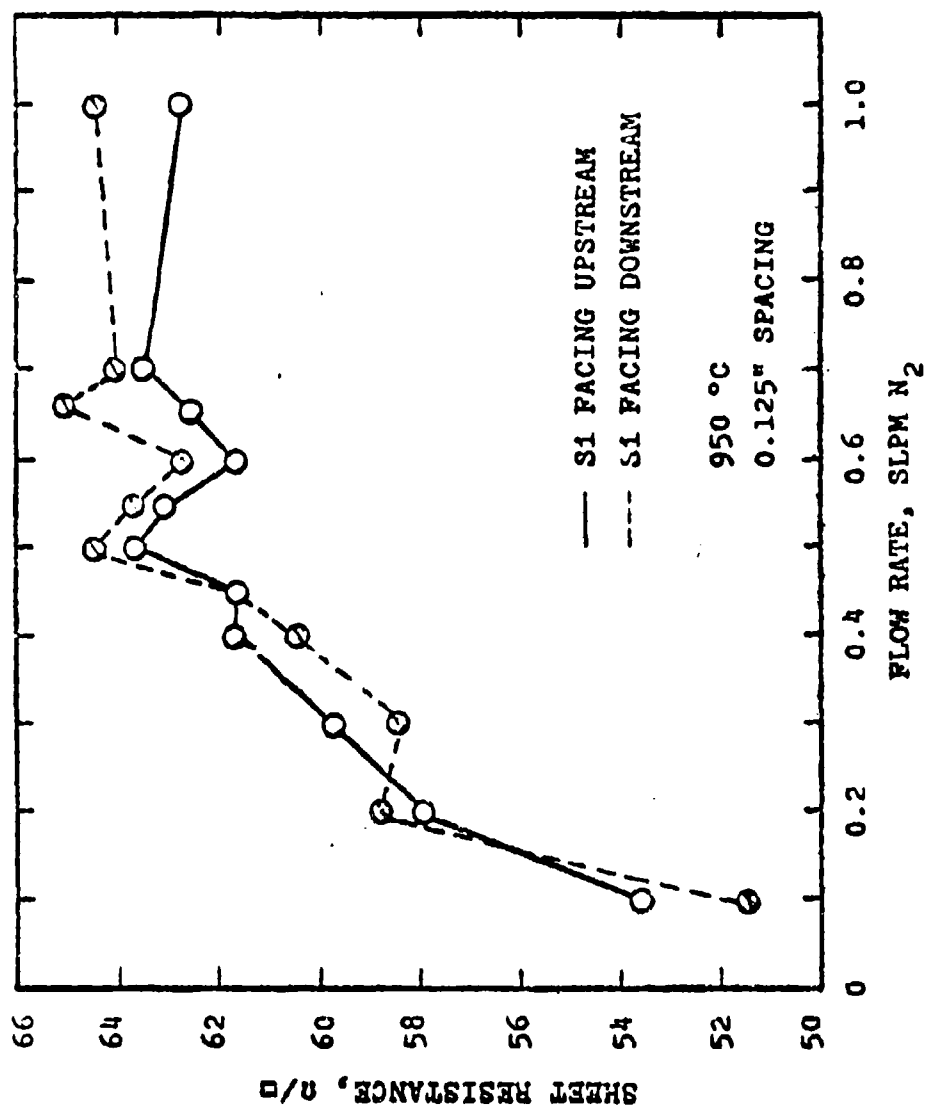


Figure 7 - Sheet Resistance Versus Flow Rate

where

- J - time averaged diffusion flux per unit cross-section
- \bar{D} - time averaged diffusion coefficient
- X_A - time averaged molar concentration of diffusing species
- X - distance coordinate.

Examination of the data suggests mass transport dominated by concentration gradient diffusion. Support of the dominance of mass transport by concentration gradient diffusion rather than bulk movement is found in that at any given flow rate the difference in sheet resistance readings for silicon wafers facing upstream and for those facing downstream is relatively insignificant. A minimum difference was observed for 0.45 slpm and all subsequent diffusion work was performed at this flow rate.

The influence of gas ambient was also studied and Figure 8 shows the sheet resistance vs. time for nitrogen, argon, and helium ambients. The effect of spacing between BN and silicon wafers was also studied. Figure 9 shows the diffusion boat arrangement for the spacing experiment the variation of sheet resistance with spacing is shown in Figure 10. An apparent paradox appears to exist upon examination of Figure 8 and 10. For diffusion controlled mass transport one would expect

- (a) increasing sheet resistance (decreasing total number of impurity atoms) as the

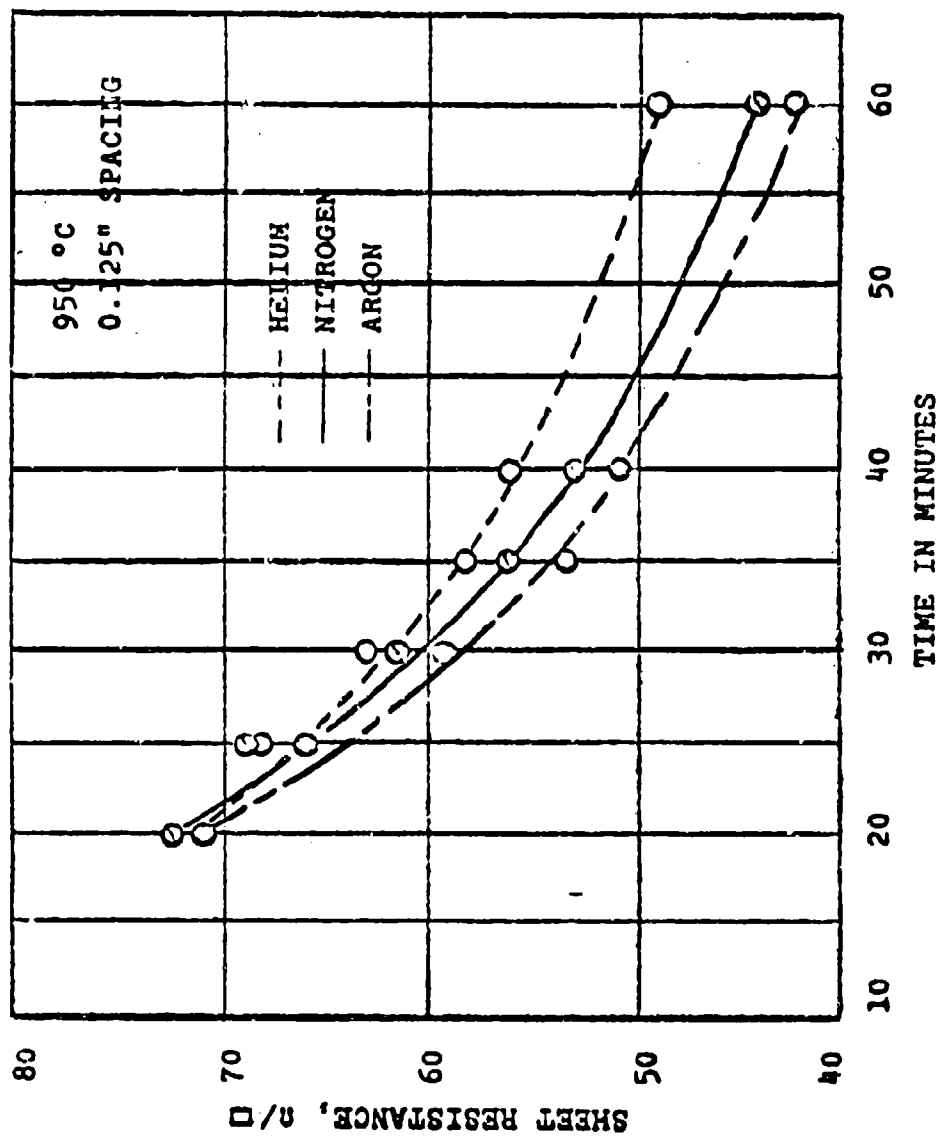


Figure 8 - Sheet Resistance Versus Time and Ambient

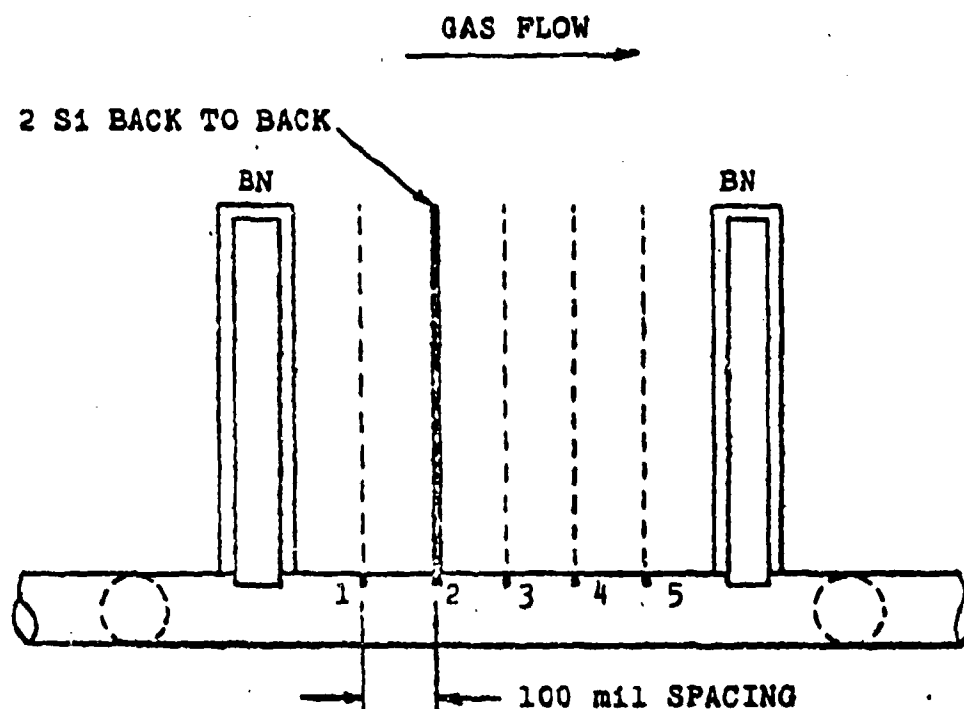


Figure 9 - Positional Relationship Between Silicon and BN for Sheet Resistance Versus Spacing

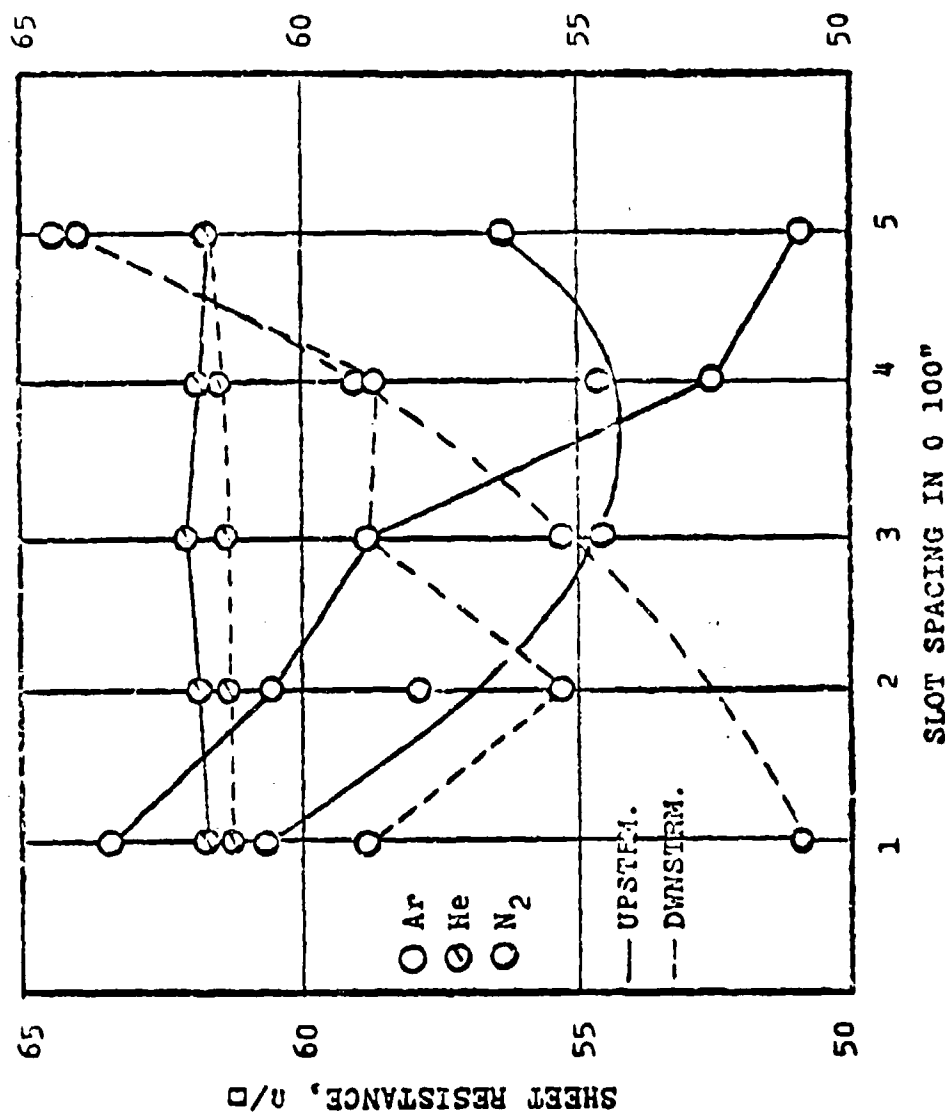


Figure 10 - Sheet Resistance Versus Spacing

spacing from source to silicon wafer increases, and

- (b) decreased sheet resistance as the diffusion coefficient of the transported species increases for lighter gases. It can be seen that Figure 8 and 10 indicate the opposite effects.

In order to gain more insight into this apparent paradox silicon wafers used in obtaining the upstream data for argon and helium ambients were divided into equal halves. One group was subjected to ellipsometric measurements (9) and the other group was subjected to impurity profiling. To insure that a minimum of oxide was present when the ellipsometric measurements were made, the silicon wafers and a control wafer (undiffused) were stripped of any oxide by immersion in concentrated HF for one minute. Measurements obtained with the ellipsometer were compared to measurements made on an undiffused silicon wafer and data obtained by Vedam and So (10). Since ellipsometer measurements are extremely accurate in determining thin films on the order of a monoatomic layer (11) and even small deviations in ψ , amplitude ratio, and Δ , relative phase change, from the true values are indicative of a thin oxide layer or surface phase. Previous investigation (12) have used ellipsometric measurements as evidence of the formation of a Si-B phase at the silicon surface as the

result of heavy diborane doping. Using a similar approach the ψ and Δ measurements differing from that obtained for the control silicon wafer are interpreted as indicative of various thicknesses of a Si-B phase. The data in Table 6 reveals that, except for 500 mil spacing, the difference in the observed and control ψ and Δ measurements decreases and in turn the thickness of the Si-B phase decreases as the spacing between the BN and silicon wafer increases. The result of this decrease in Si-B phase has negligible effect upon sheet resistance versus spacing for a helium ambient but a marked effect on sheet resistance versus spacing for the argon ambient. From the data it can be hypothesized that (a) as the Si-B phase increases above a specific thickness its effect becomes saturated and the diffusion of boron into silicon becomes independent of the increase in thickness, and (b) below this saturation thickness the diffusion of boron in silicon becomes dependent upon the thickness of the Si-B phase.

Impurity profiles for helium ambient depositions shown in Figure 11 tend to verify the hypothesis (a) by the duplication of profiles for 100, 200 and 500 mil spacings. The wafer corresponding to a 300 mil spacing broke during profiling and the profile for the 400 mil spaced wafer is felt to be experimentally incorrect because of the discrepancy between calculated sheet resistance from profile $\rho_s = 55$ ohms square, and the measured sheet resistance $\bar{\rho}_s = 61.3$ ohms square.

Table 6 - Ellipsometric Data for Various Spacings During Diffusion

SPACING	ARGON				HELIUM			
	$\bar{\rho}_s$	x_j	τ	Δ	$\bar{\rho}_s$	x_j	τ	Δ
0.100 ^m	65.6 n/	3200 \AA	12.11	167.63	62.5 n/	2600 \AA	^{††} 20.56	100.91
0.200	59.0	3300	**	**	61.7	2600	[†] 16.38	119.11
0.300	58.7	3500	12.03	169.99	62.9	3300	13.56	140.92
0.400	55.4	3750	11.97	172.29	61.3	**	13.48	143.44
0.500	58.5	**	12.10	169.61	60.5	2600	13.81	137.97
CONTROL	-	-	12.01	173.92	-	-	12.01	173.92
TRUE*	-	-	11.83	172.48	-	-	11.83	172.48

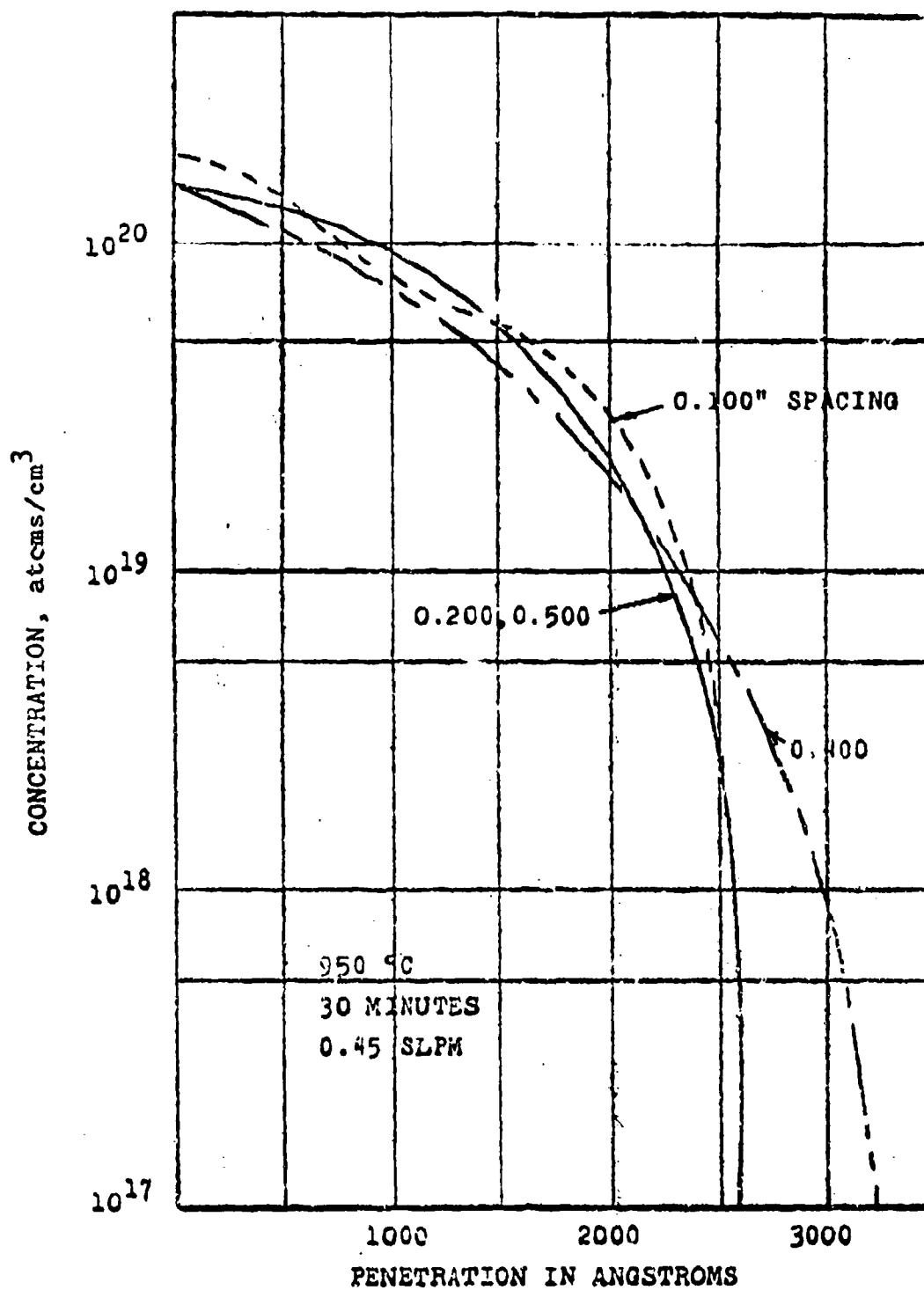


Figure 11 - Helium Ambient Impurity Profile

For depositions done in a large ambient figure 12 shows the impurity profile for various spacings. The data suggests that as the distance between source and silicon increases the junction depth increases and sheet resistance decreases. For a constant deposition time and temperature an increase in junction depth dictates an increase in diffusion coefficient. The influence of boron concentration upon boron diffusion has been considered by many investigations (13, 14, 15, 16, 17, 18). The variation of diffusion coefficient with doping level was calculated for high temperature diffusions and is discussed later in this report.

Experiments were conducted at elevated temperature to study the gas flow rate and system geometry effects. Figure 13 shows the flow rate dependence on sheet resistance at 1100°C and Figure 14 shows the flow rate dependence on sheet resistance at 1200°C . The diffusions were for 30 minutes with a 95% N_2 and 5% O_2 ambient. It can be seen in Figure 13 that for very low flow rates the sheet resistance was very high and that for the condition of zero flow rate the sheet resistance was one order of magnitude higher than with gas flow. This indicates that the effect of flow rate on sheet resistance is complex and not readily explainable. The influence of spacing on sheet resistance is shown in Figure 15. The diffusion boat arrangement for these experiments were similar to that

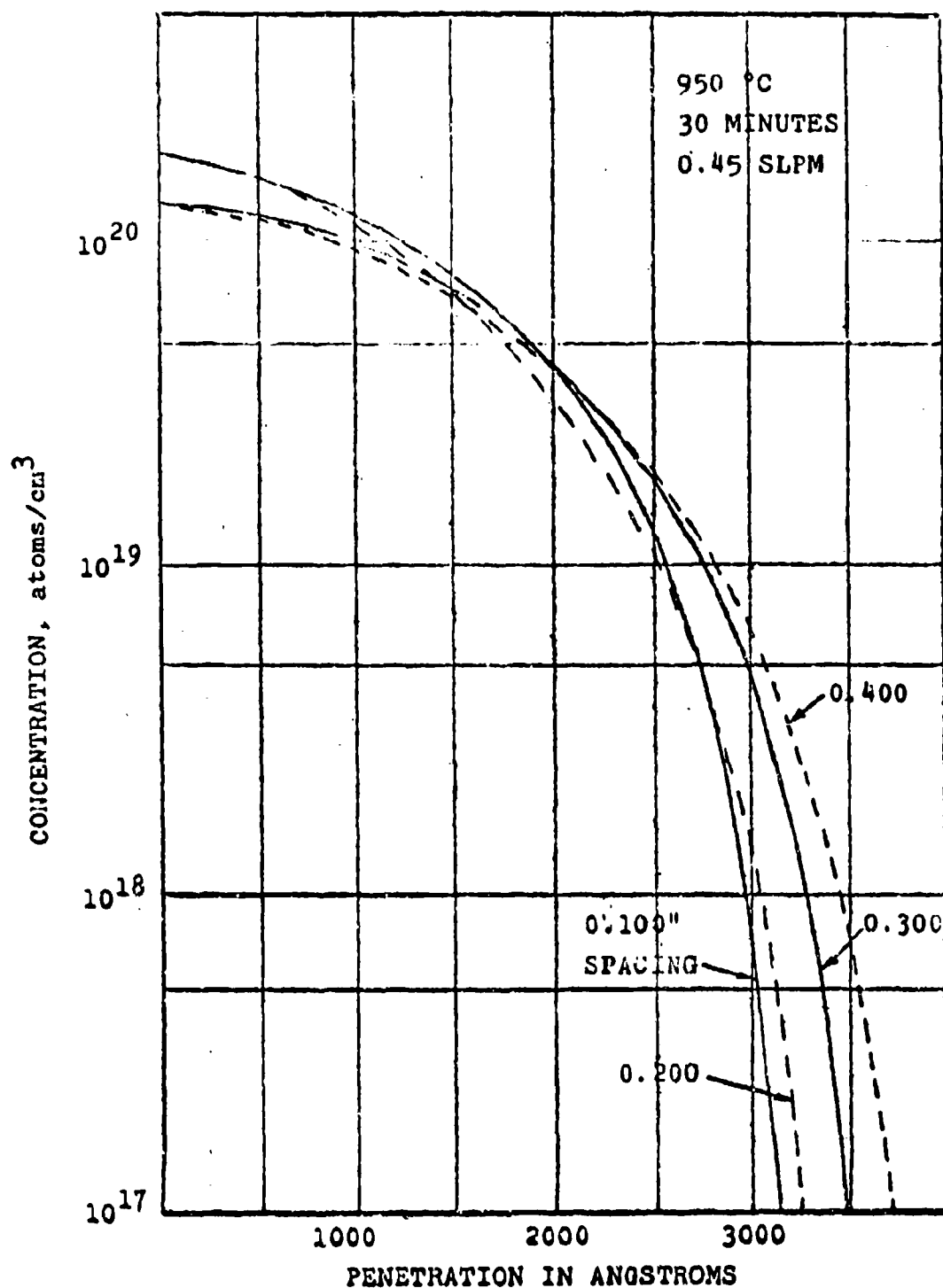


Figure 12 - Argon Ambient Impurity Profile

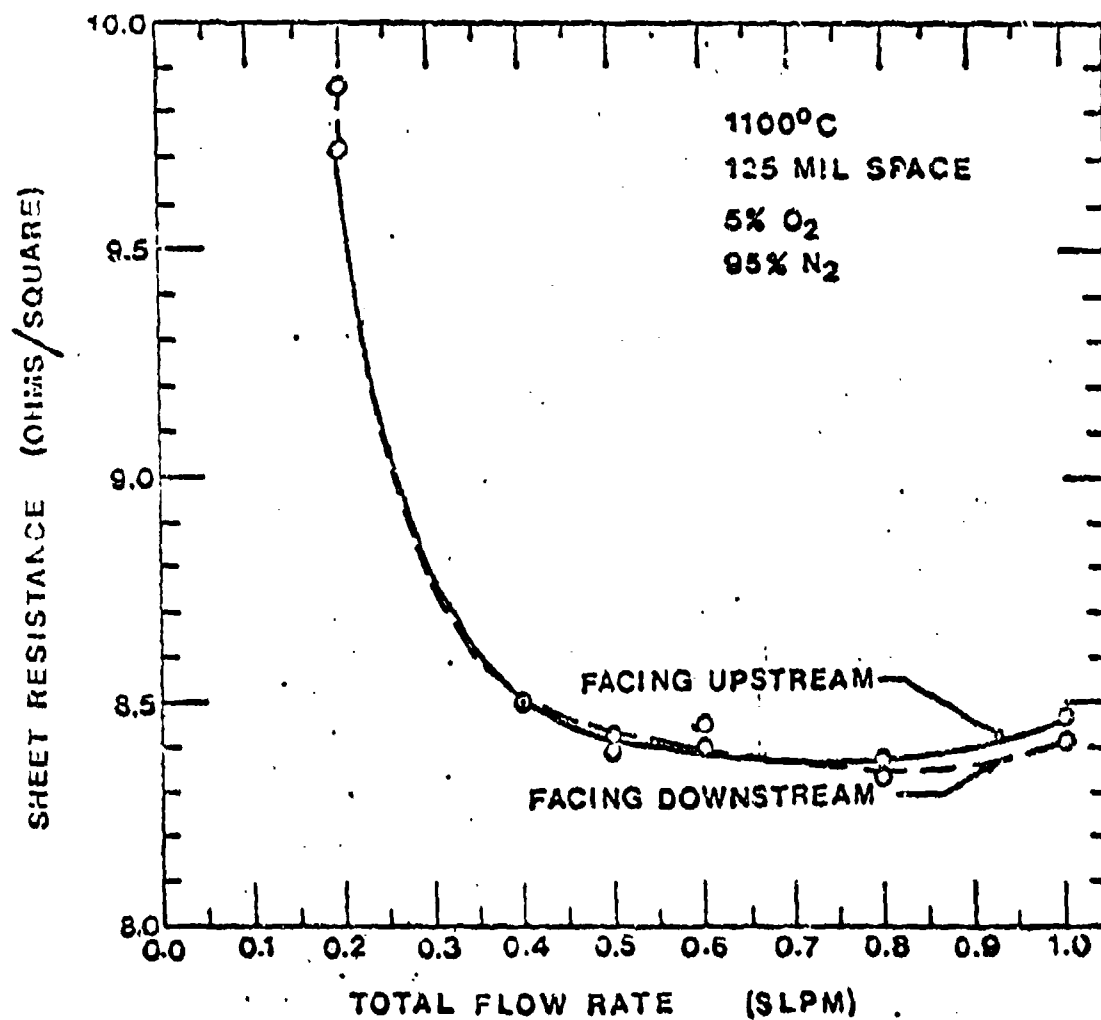


Figure 13 - Sheet Resistance versus Flow Rate For 1100°C Diffusions

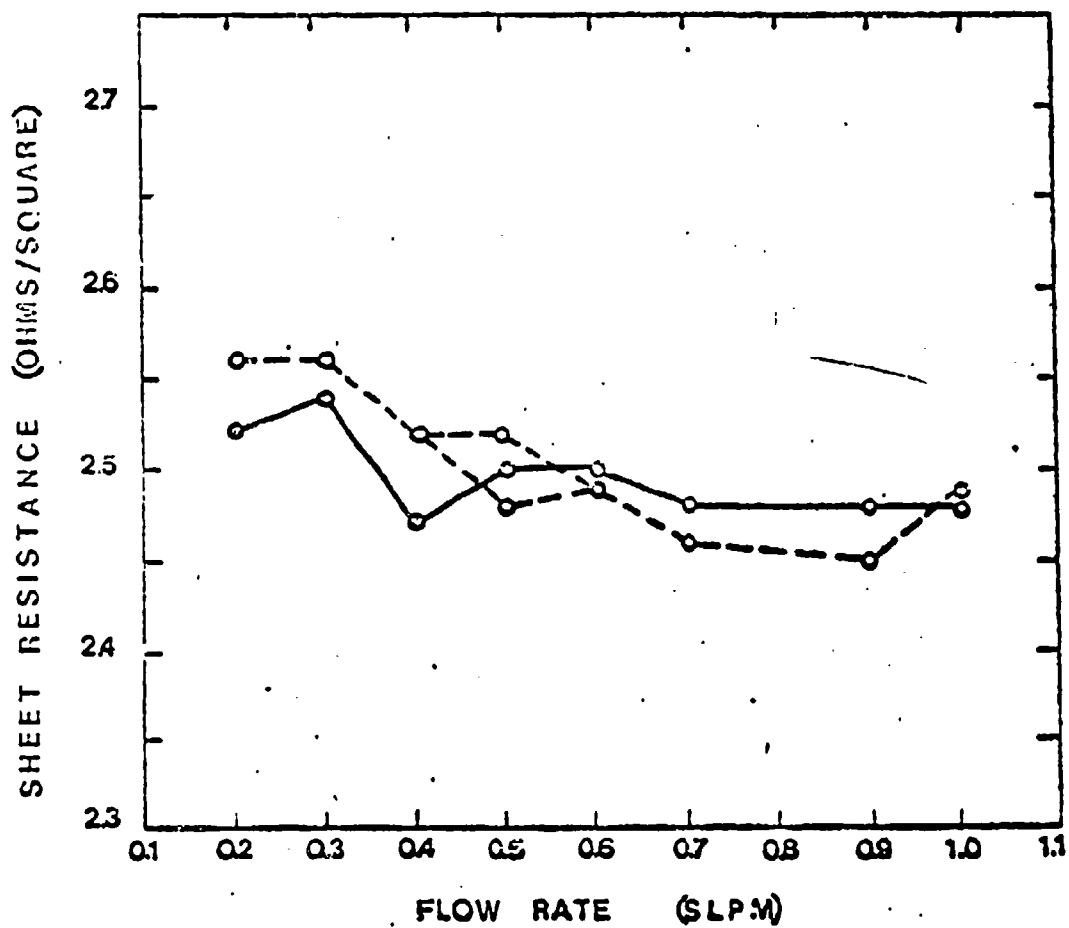


Figure 14 - Sheet Resistance versus Flow Rate For 1200°C Diffusions .

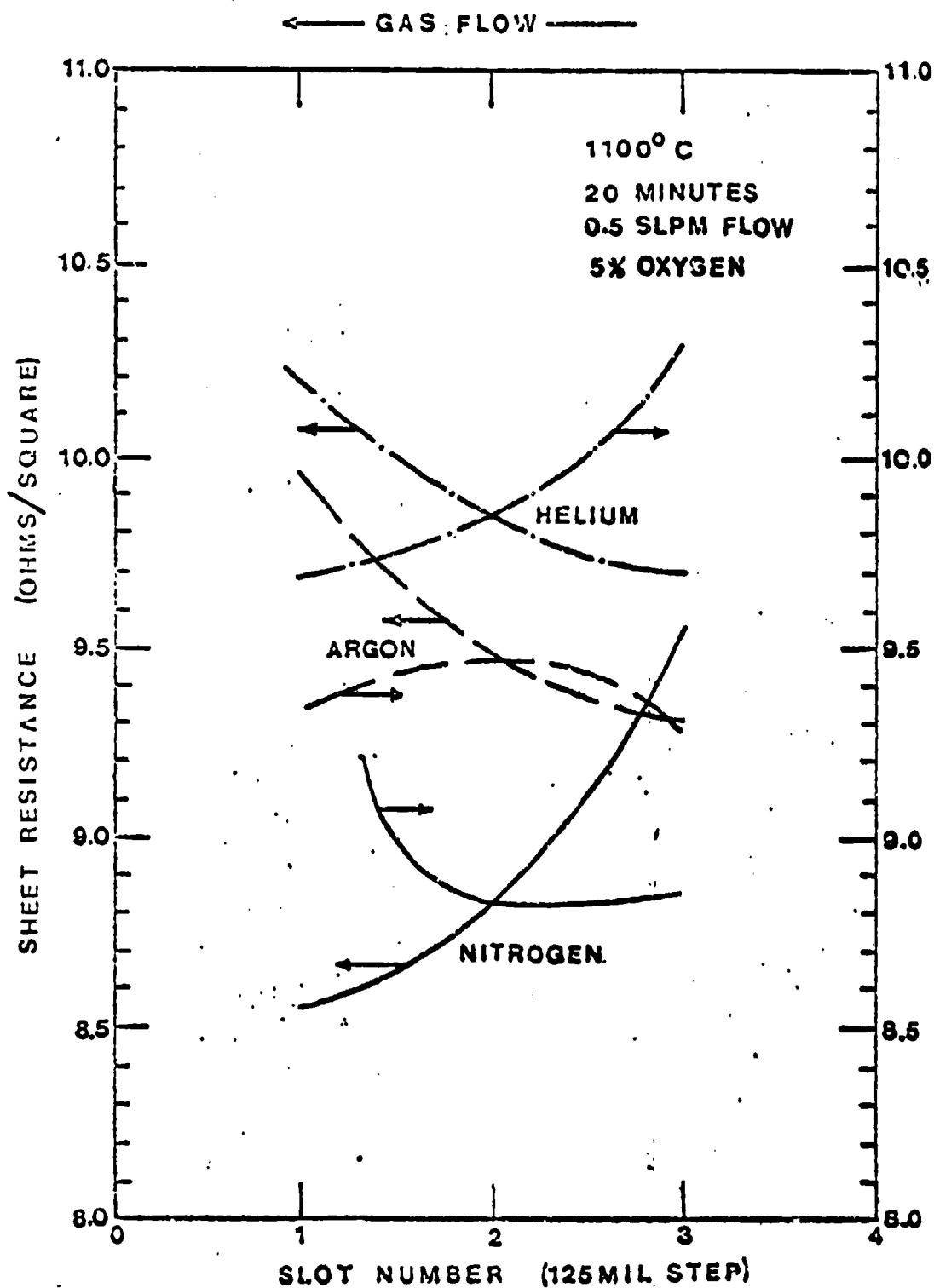


Figure 15 - Sheet Resistance versus Spacing with Gas Ambient as a Parameter

shown in Figure 9. It can be seen that in order to achieve uniform diffusions in silicon wafers facing upstream and downstream the silicon wafers should be spaced equidistant from the BN wafers. This supports the results obtained at lower temperatures and indicates that the assumption of a concentration diffusion mass transport is plausible. There is an obvious difference in the effect of ambients which can be seen when comparing the data in Figure 15 and Figure 10 because the sheet resistance is highest in both cases for helium ambients, however, it is lowest for the N_2 ambient at 1100°C and for the A ambient at 900°C . It is possible to explain this difference using the theory of ordinary diffusion of gases at low densities (19). Using Chapman-Enskog kinetic theory to predict the diffusivity of species A in gas B it is possible to calculate the diffusivities at various temperatures. It can be shown that the diffusivity of the HBO_2 species in argon and nitrogen ambients is temperature dependent. The results of these calculations are given below:

$$\text{at } 1100^\circ\text{C} \quad D_{\text{Argon}} = 2.32 \text{ cm}^2/\text{sec}, D_{N_2} = 2.17 \text{ cm}^2/\text{sec}$$

$$\text{at } 800^\circ\text{C} \quad D_{\text{Argon}} = 1.37 \text{ cm}^2/\text{sec}, D_{N_2} = 1.57 \text{ cm}^2/\text{sec}$$

It can be seen from these results that the diffusivity of HBO_2 in argon at elevated temperatures is greater than in nitrogen but as temperature decreases the diffusivity of HBO_2 in nitrogen becomes greater than in argon. It is

because of this that it is possible to account for the difference in sheet resistance values in various ambients.

CHARACTERIZATION OF BN DIFFUSION BEHAVIOR

In order to help characterize the behavior of BN diffusion systems, studies were made of the diffusion process for temperature ranges from 850°C to 1200°C. Sheet resistance vs. time at different temperatures in a nitrogen ambient is shown for ABN in Figure 16. It can be seen that the spacing dependence discussed previously is evident. It should be pointed out that the spacing dependence of sheet resistance is an additional degree of freedom that is available in planar diffusion source systems. At temperatures above 1000°C MBN was studied and Figure 17 shows sheet resistance as a function of time at various temperatures with different ambients.

In addition to the diffusion profiles obtained at lower temperatures diffusions done at higher temperatures indicate the influence of gas ambients on profiles. Figure 18 shows impurity concentration as a function of penetration at 1100°C for 45 minutes diffusions done in helium, argon, and nitrogen. The profile data was obtained by incremental sheet resistance data and converted to impurity profile by a technique developed by Donovan (20). Computer techniques were utilized to aid in the numerical computations. The silicon layers were removed

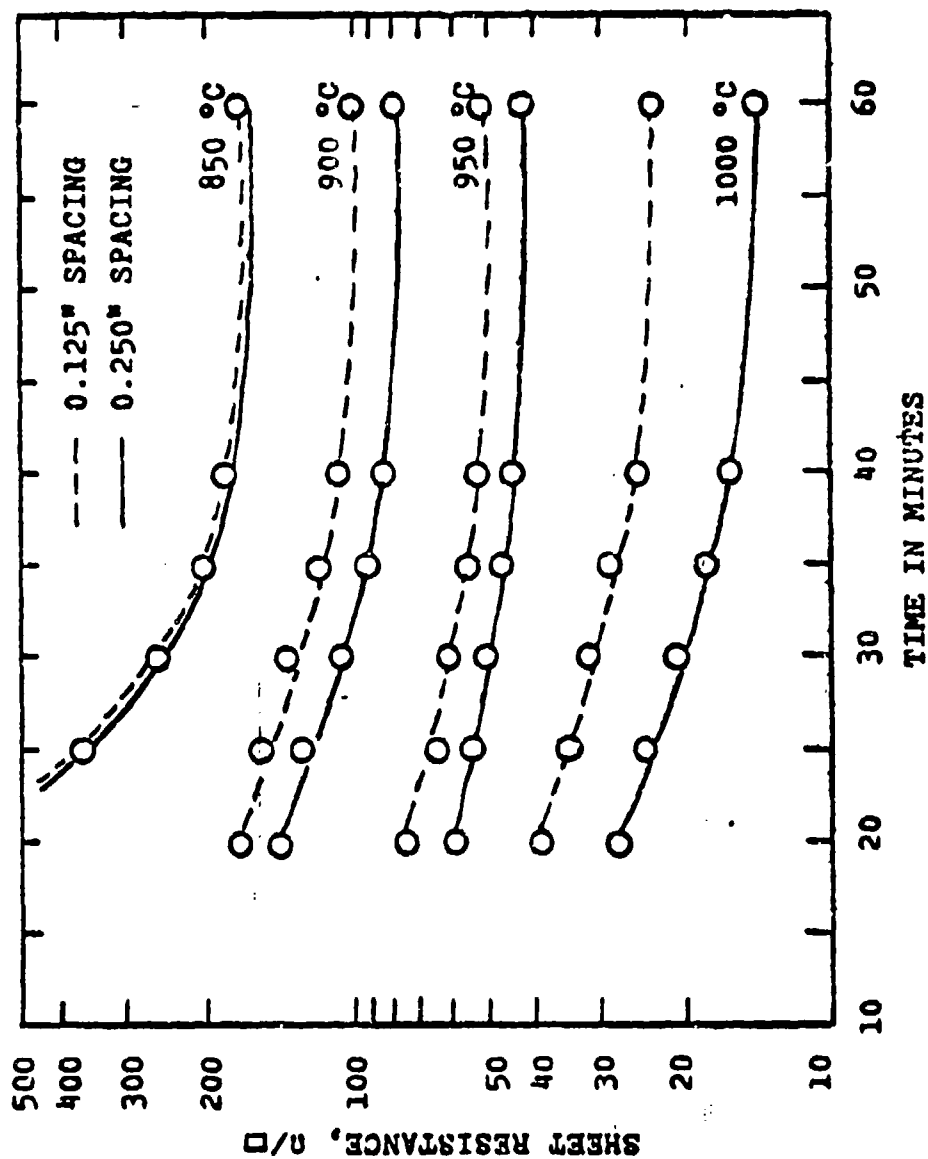


Figure 16 - Sheet Resistance Versus Time, Temperature and Spacing

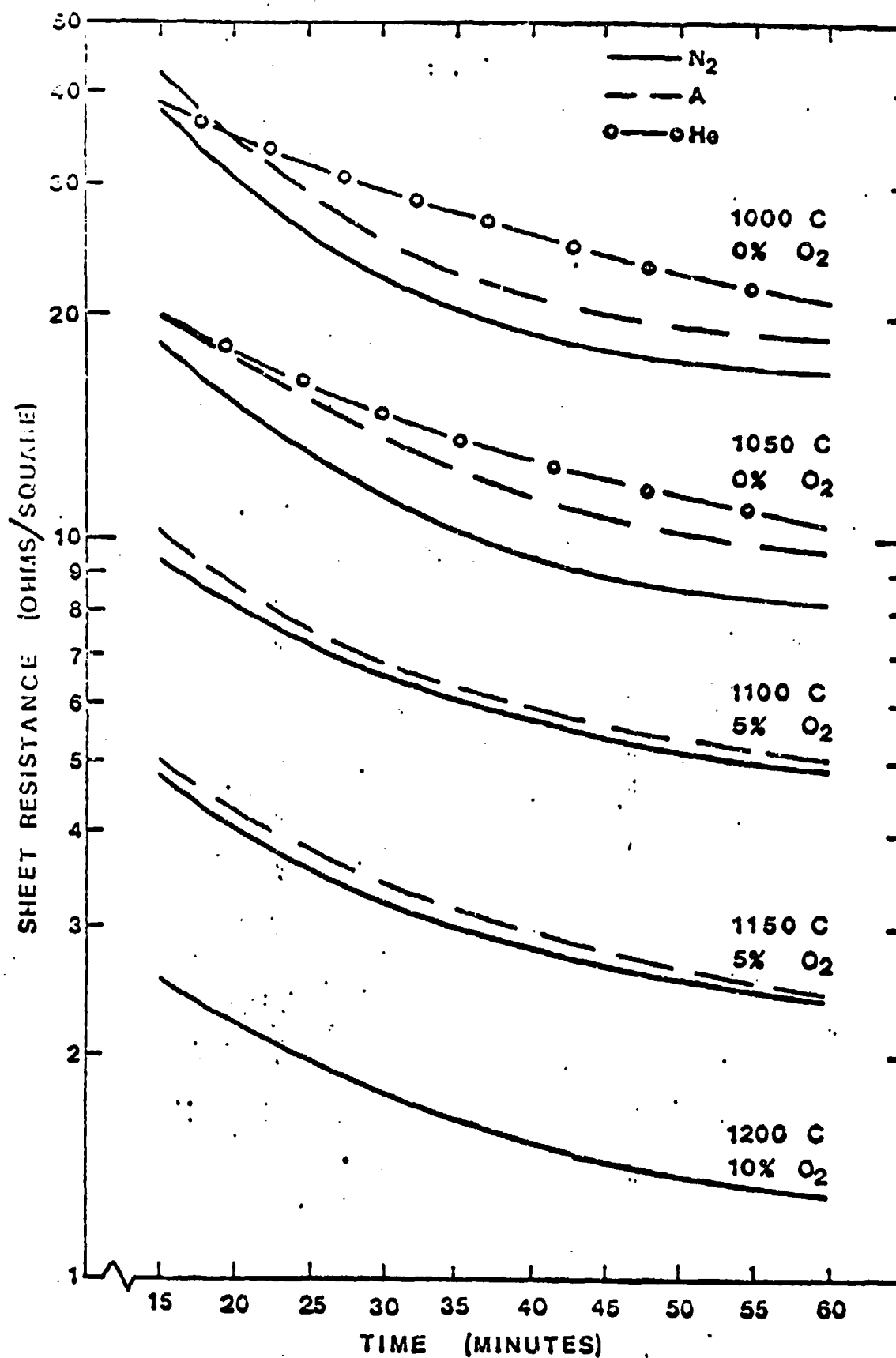


Figure 17 - Sheet Resistance versus Time From 1000°C to 1200°C in Various Ambients

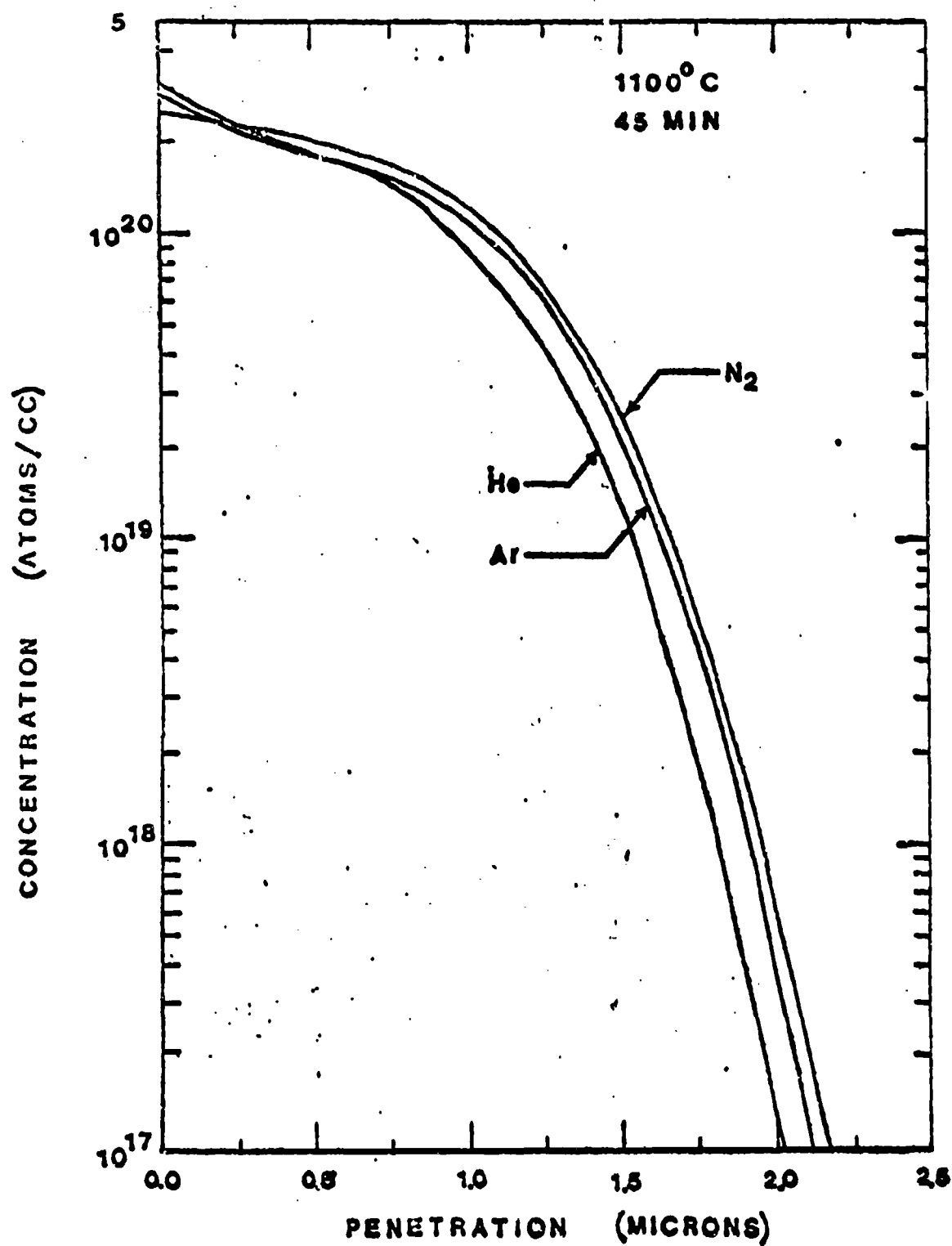


Figure 18 - Diffused Impurity Profile Showing the Effects of Inert Gas Ambient

by anodic oxidation of silicon in a 0.04 KNO_3 in ethylene glycol (21). The correlation between forming voltage and oxide thickness was determined by interferometry and the use of a UV-Visible spectrophotometer (22). The diffusion profile data indicates that the ambient conditions can influence junction depth significantly. Here again the role of the Si-B phase formed on the surface of the silicon wafer appears to be the controlling factor. The heaviest glass formation on the silicon surface occurs during diffusions done in a helium ambient and the lightest glass formation occurs in nitrogen. Since profiles are measured after complete glass removal the difference in junction depth could be accounted for by the amount of silicon consumed during the glass formation and subsequently removed during the glass removal step. One can account for this mathematically by considering the diffusion into a medium with the boundary moving in the direction of diffusion. Using this approach it is possible to show that for these high boron concentrations the junction depth is reduced because of the moving boundary. (30)

The reproducibility of diffusion processes on a run to run basis were studied using ABN and MBN. In addition the effect of flow rate on reproducibility was also studied for nitrogen and argon. Figures 19 and 20 show the run to run sheet resistance variation in nitrogen and argon at two different flow rates for 30 minutes diffusion at 950°C

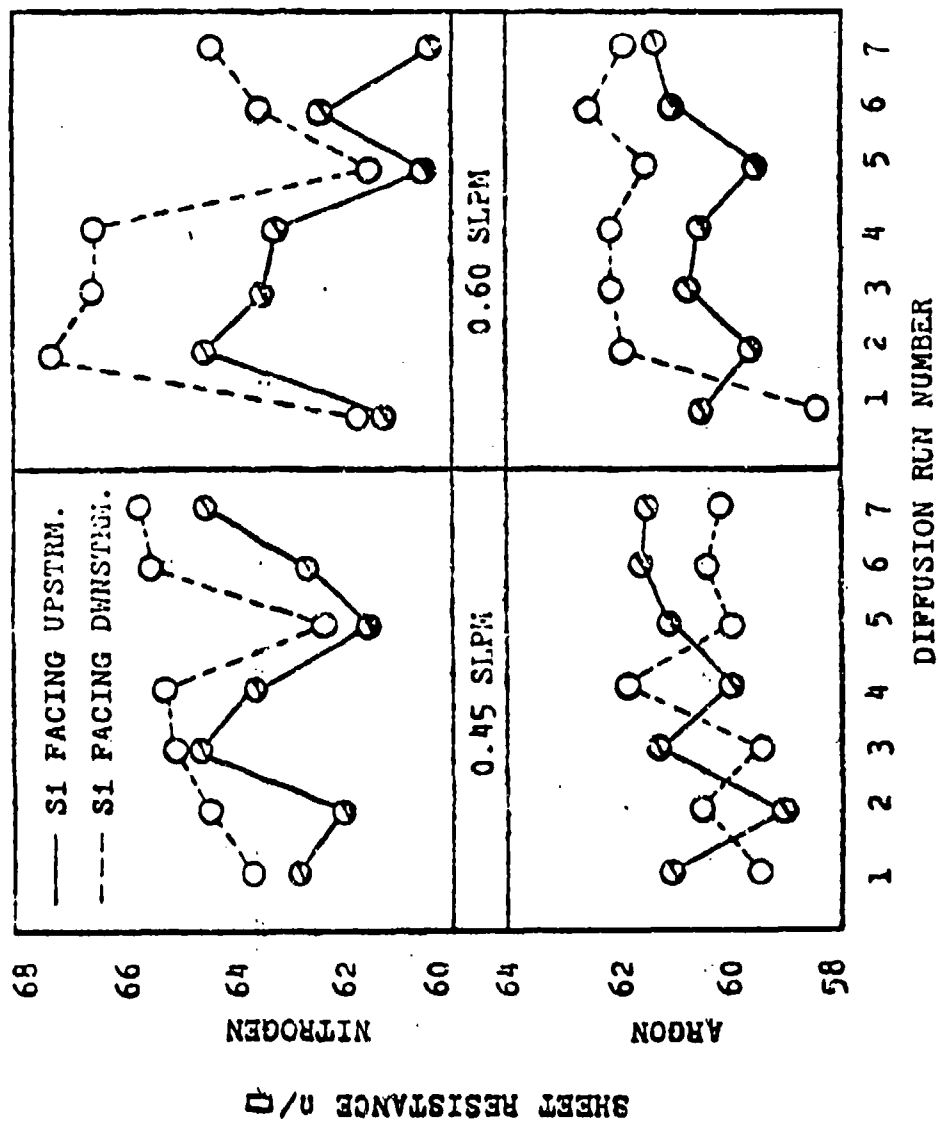


Figure 19 - Sheet Resistance Versus Run Number

1150° C
30 MIN

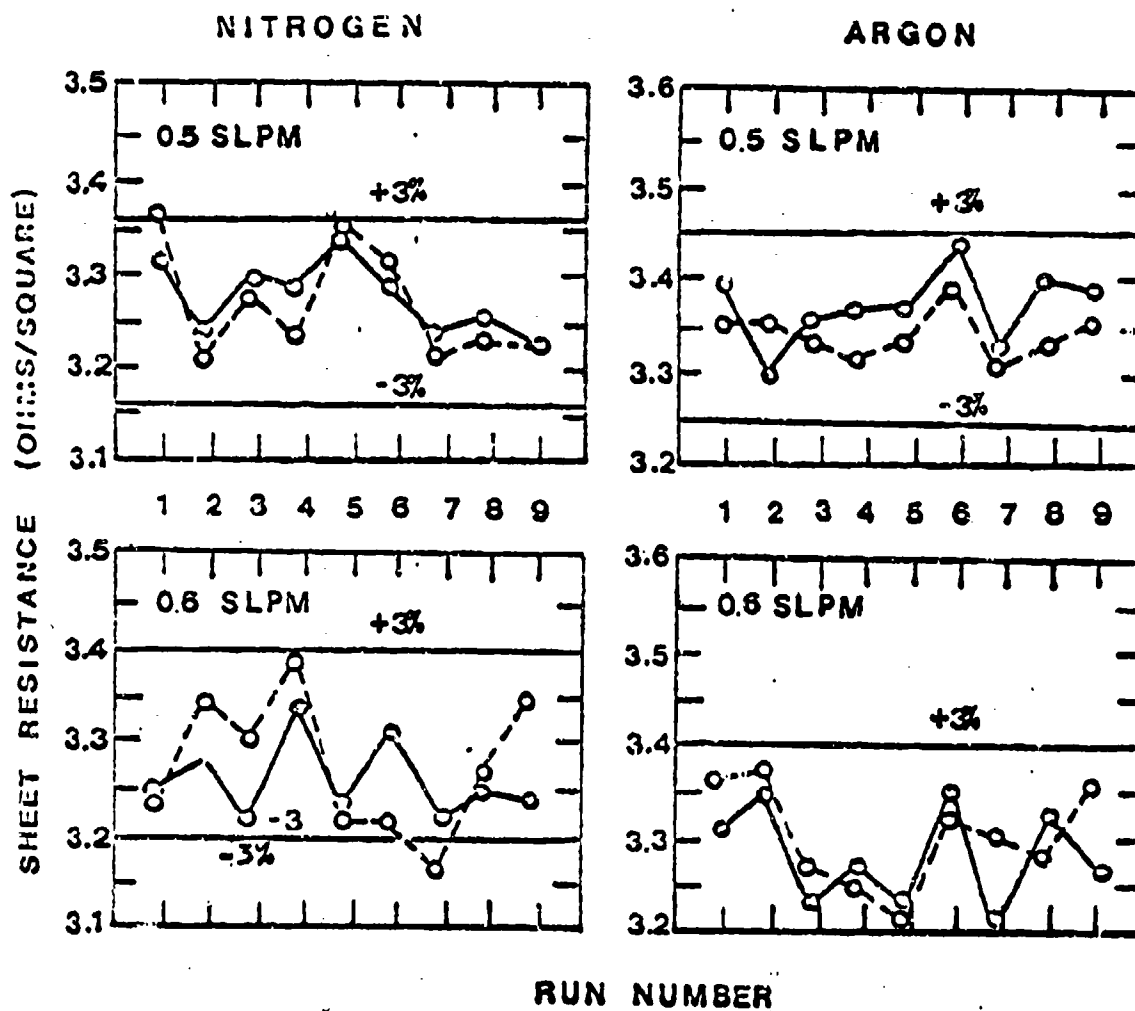
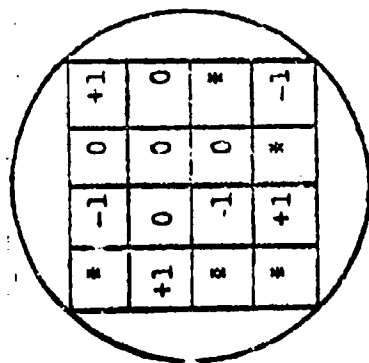


Figure 20 - Reproducibility of Sheet Resistance from Run to Run with Gas Ambient and Flow Rate as Parameters

and 1150°C respectively. Examination of the data reveals improved run to run sheet resistance uniformity for lower flow rates and lower thermally conductive gas ambients. The primary mechanism of heat transfer at typical diffusion temperatures is by radiation (23) and although the emitted energy is significant the absorbant capacity of silicon is comparable to the cooling capacity of gases (24). Because of this it is expected that better reproducibility is achievable for lower flow rates and lower thermally conductive gases, argon as compared to nitrogen.

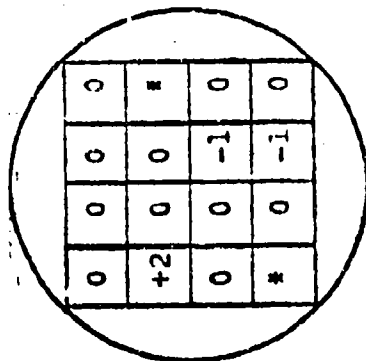
Diffusion uniformity across a silicon wafer was determined for randomly selected silicon wafers used in previous studies. Figures 21, 22, 23 and 24 show resistance across a silicon wafer in various ambients. The data in Figure 21 is for 30 minute diffusion at 950°C . The numbers in the wafer map indicate the % deviation from average across the wafer sheet resistance. The mappings were obtained by scribing the silicon wafers into 250 mil squares, which is comparable to LSI chip size, and four point probe measurement made on each chip. For all ambients the indicative sheet resistance variation is of the order of 1-2%. Previously reported capabilities of open tube diborane system (25) and capsule systems (26) are respectively $\pm 4\%$ and $\pm 3\%$. From this data it can be seen that planar wafer sources are attractive diffusion sources for LSI processing because of the high uniform diffusions that are achieved.

* sample broke from scribing



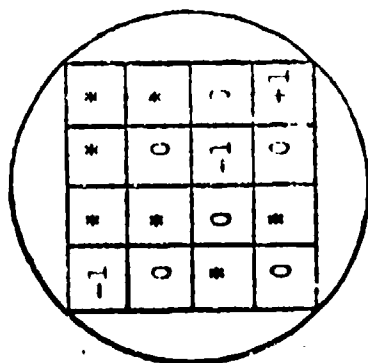
*	-1	0	+1
+1	0	0	0
*	-1	0	*
*	+1	*	-1

HELIUM



0	0	0	0
+2	0	0	*
0	0	-1	0
*	0	-1	0

ARGON



-1	*	*	*
0	*	0	*
*	0	-1	0
0	*	0	+1

NITROGEN

Figure 21 - % Sheet Resistance Variation Across Silicon Wafer

1100°C

60 MIN

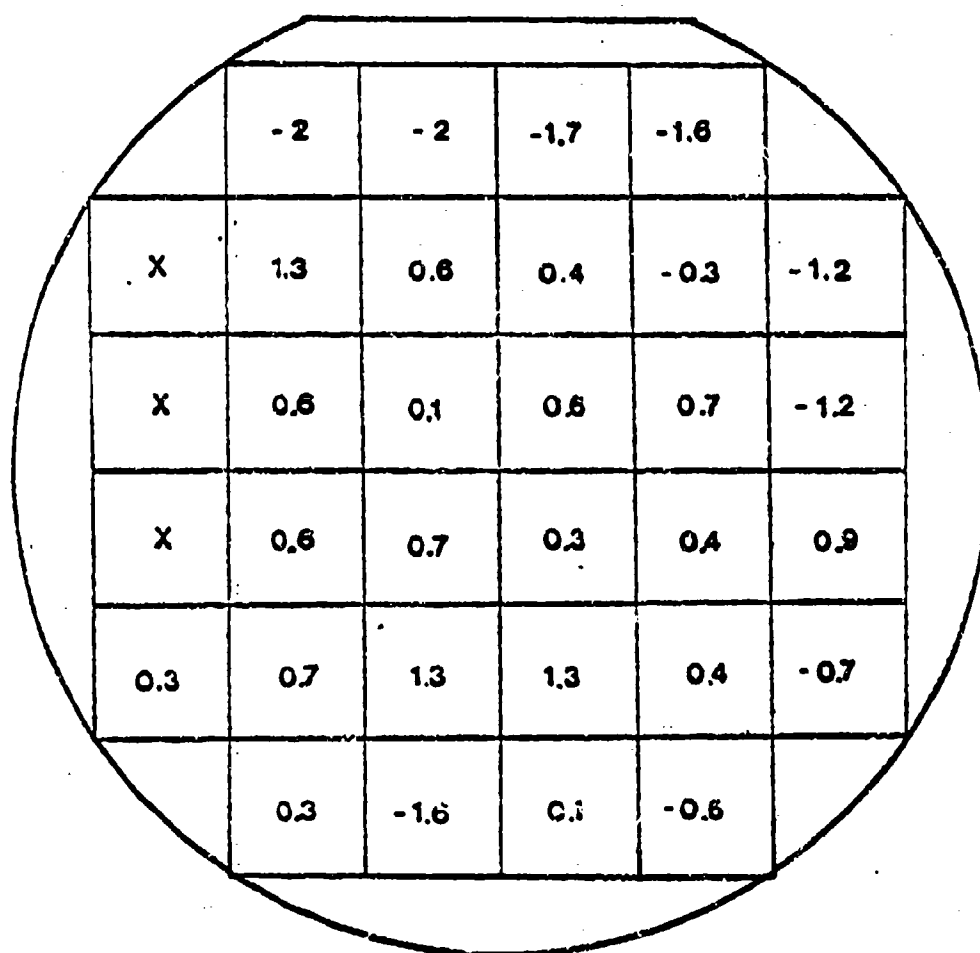
0.475 SLPM N₂0.025 SLPM O₂

Figure 22 - Across Wafer Uniformity at 1100°C for
Diffusions Done in a Nitrogen Ambient

1100°C

60 MIN

0.475 SLP Ar

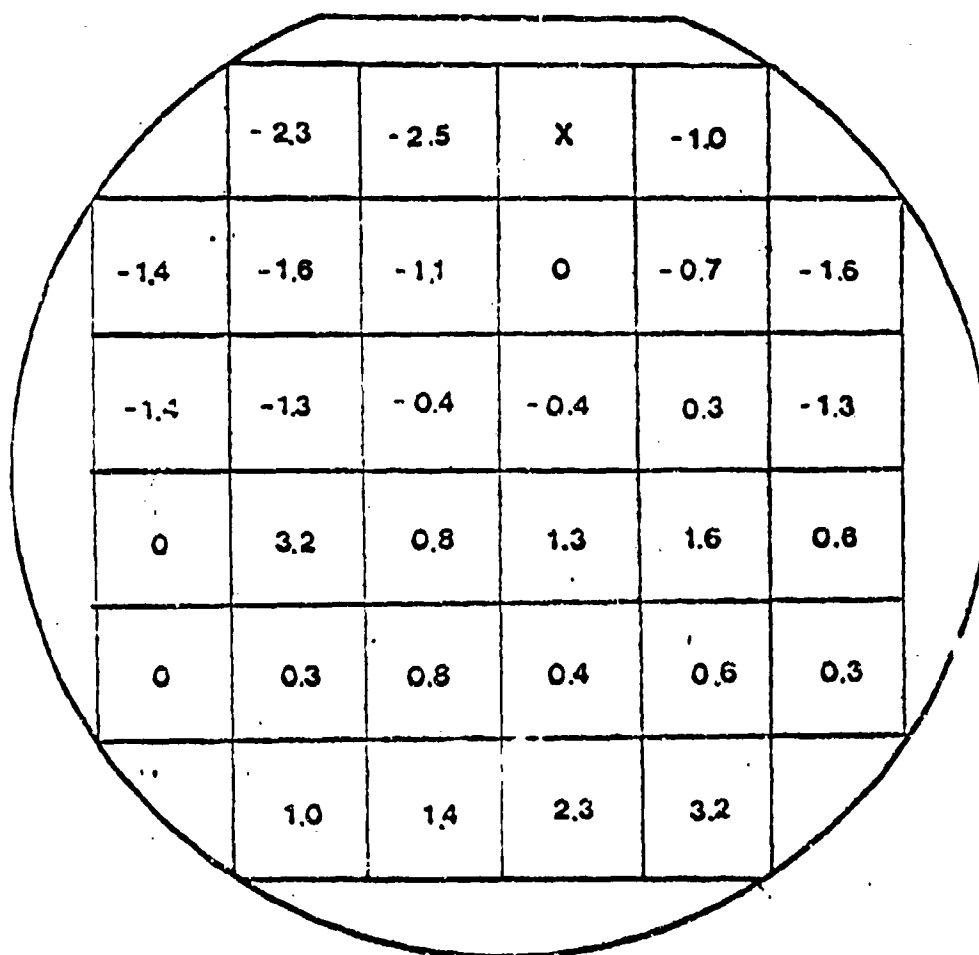
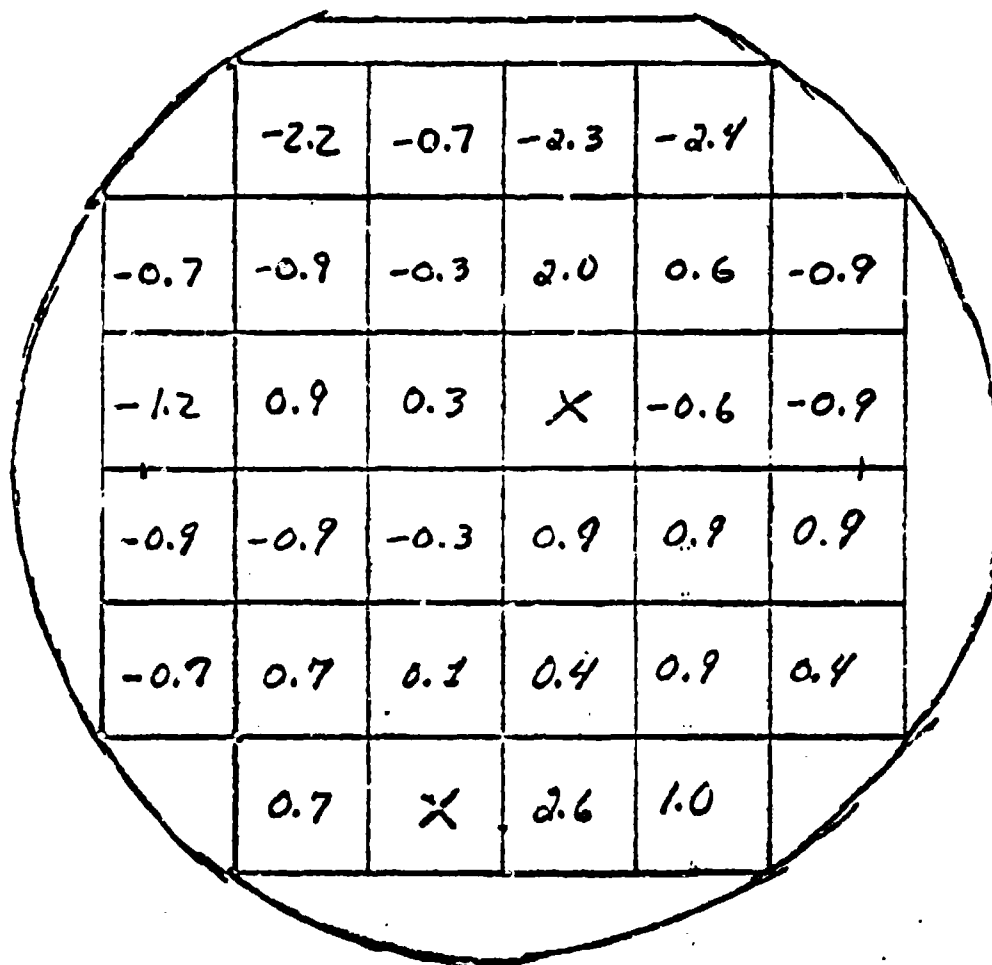
0.025 SLF O₂

Figure 23 - Across Wafer Uniformity of Sheet Resistance
for Diffusion at 1100°C in an Argon Ambient

1100° C
60 MIN
Helium



* X indicates a broken square.

Figure 24 - Percentage Variation of Sheet Resistance Across the Wafer Area for Diffusions at 1100°C in a Helium Ambient.

BN SOURCE COMPOSITION

An effort was made to determine whether certain variables in the BN manufacturing process had any influence on its performance as a diffusion source and also whether a compositional change might be needed to optimize BN's performance as a diffusion source.

The principal manufacturing process variables have been density of the ABN and its B_2O_3 binder concentration. Figure 25 and 26 show log-log plots of TGA data for material varying in density from 1.96 to 2.01 gm/cm³ and B_2O_3 binder concentration from 2.08 to 8.98%. Examination of Figure 25, % Weight Increase for 93% BN as a Function of Wafer Density for Constant Binder Concentration of 5.38%, reveals that the slope of the oxidation curve is independent of wafer density. As indicated previously the rate of "oxide" growth can be represented as

$$W_I = at^b$$

where

W_I = % weight increase of 93%
BN in O_2

t = time in hours, and

a, b = empirical constants

For a B_2O_3 binder concentration of 5.38%, $b=0.76$ and the effect of increasing density is a decreasing value of a . While the single TGA's presented are inconclusive a

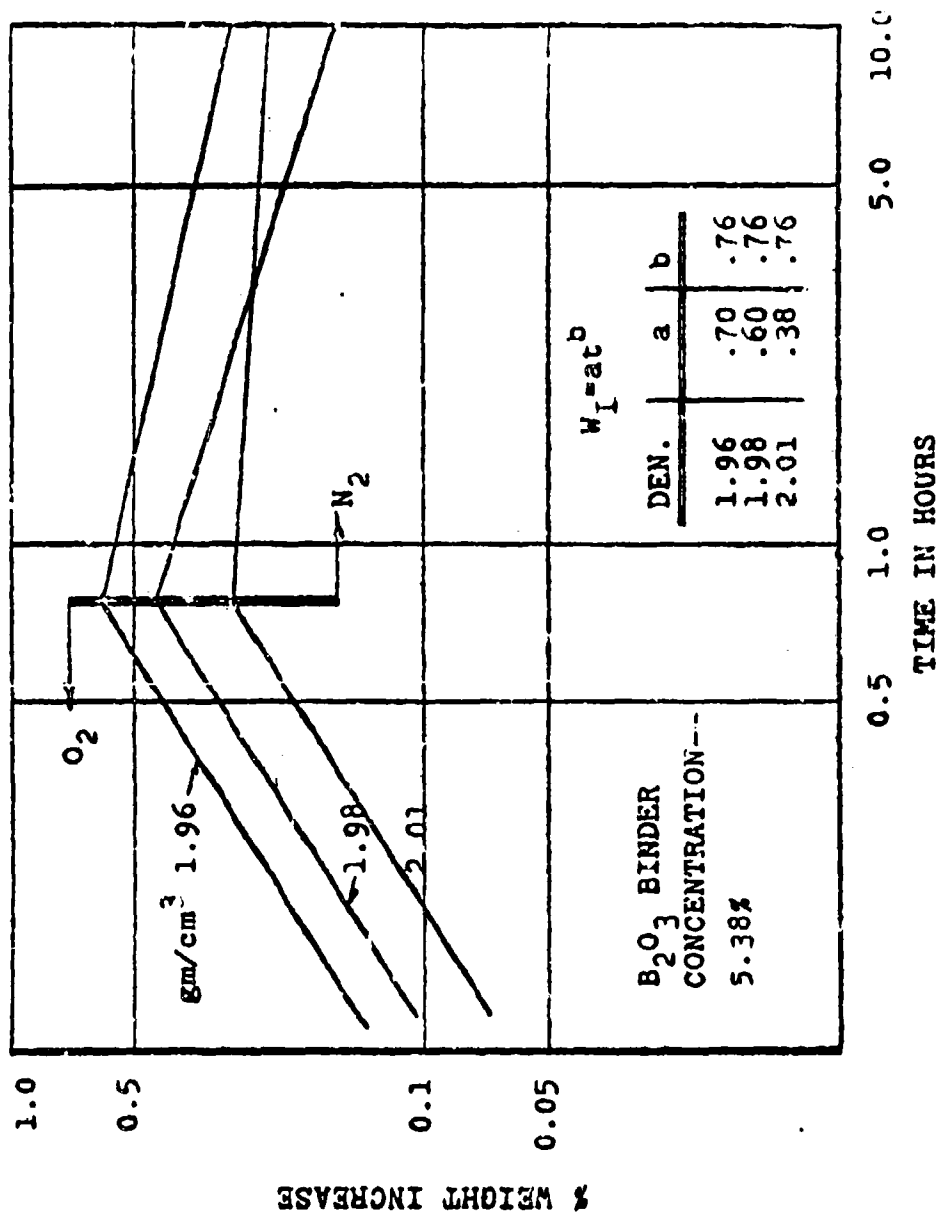


Figure 25 - Log-Log Plot of % Weight Increase as a Function of Time, Ambient and BN Wafer Density

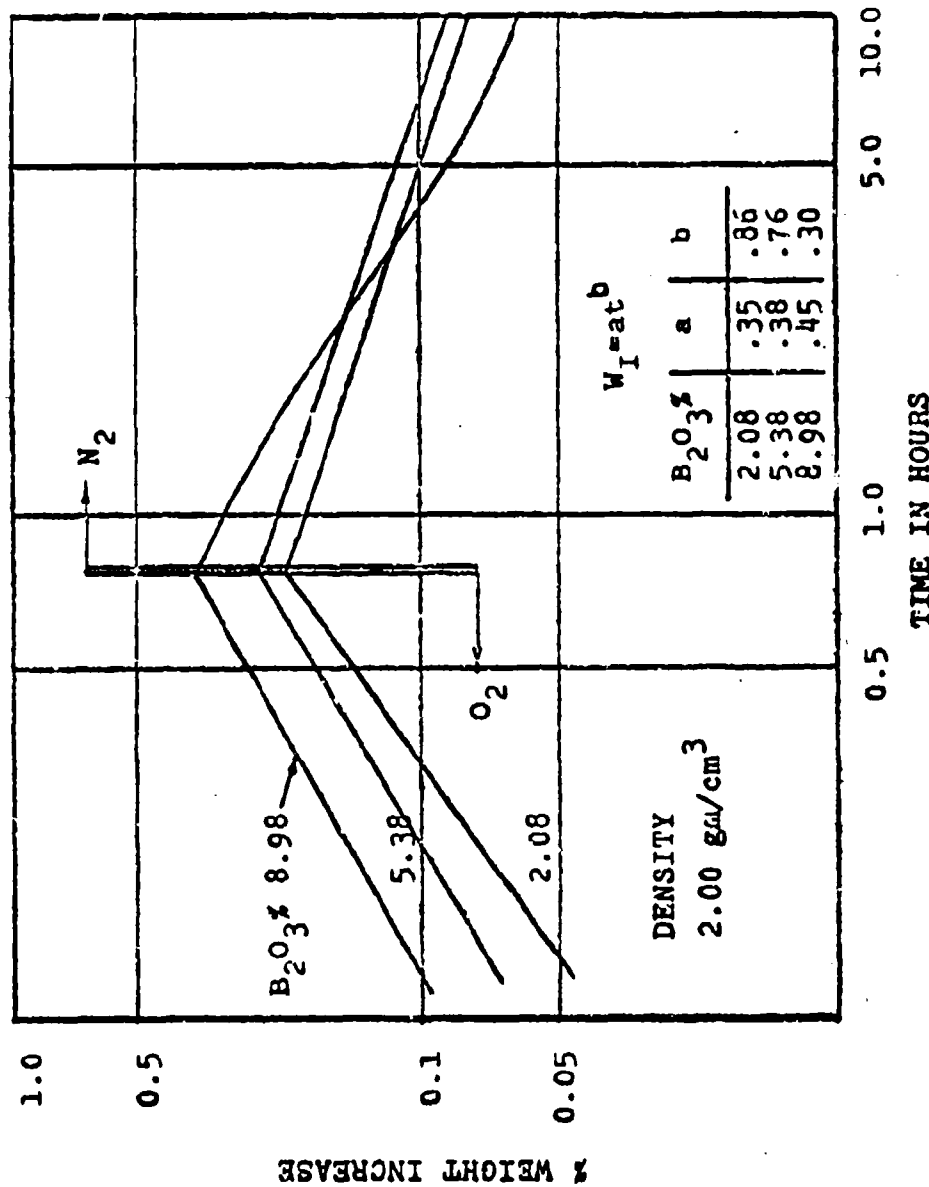


Figure 26 - Log-Log Plot of % Weight Increase as a Function of Time, Ambient and B_2O_3 Binder Concentration

possible explanation for the observed inverse relationship between density and constant a can be derived by recognition that the volatilization rates for the lower density material are larger and that the volatilization rate for pure B_2O_3 should be independent of density. Randall and Margrave (27) have demonstrated that the volatilization of B_2O_3 in the presence of water vapor is strongly dependent upon the concentration of water vapor present. While the growth of oxidized BN appears to be reaction rate limited it is conceivable that chemi-absorption of water vapor is diffusion limited. For this assumption a lower density material would pose less impedance to diffusion of a species and gain more weight due to water vapor absorption during the oxidation cycle; hence, the observed variations in volatilization rates.

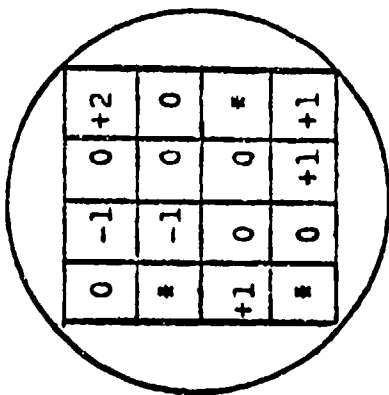
While the oxidation rate was not noticeably affected by changes in density, inspection of Figure 26, % Weight Increase for 93% BN as a Function of B_2O_3 Binder Concentration for Constant Wafer Density, indicates an oxidation rate dependence upon B_2O_3 binder concentration. At this time no reasonable explanation for the observed effects of binder concentration on constants a and b can be put forth although some wafer vapor relationship is suspected. Material with high B_2O_3 binder concentration (>5%) tends to delaminate and spall upon furnacing prior to oxidation. Discussions with Carborundum engineering

staff (28) have indicated this probably to be the result of trapped water vapor not easily removed during a drying cycle.

In light of the suspected diffusion coefficient dependence of boron in silicon on the formation and thickness of a Si-B phase it would be inappropriate to say that the effect of varying material composition would have negligible effect upon deposition performance. Within the confines of the material investigated no noticeable dependence of sheet resistance on major material composition was observed. A brief investigation of hot pressed BN body consisting of 20% SiO_2 and 80% BN significantly demonstrates the effect of reduce volatilization. Assuming an ideal solution between the oxidized BN and the SiO_2 , Raoult's Law predicts a decrease in vapor pressure of the volatile species by the mole fraction reduction. For non-ideal solutions and significantly reduced chemical activity, the vapor pressure of the volatile species is reduced even more.

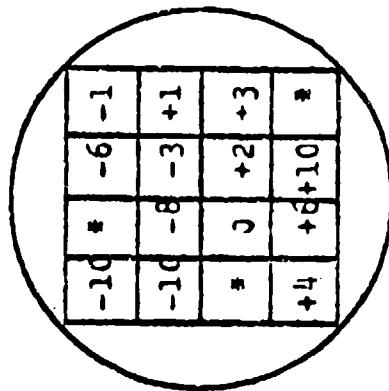
Ellipsometric measurements of diffused silicon for 20% SiO_2 /80% BN were not available and whether or not a Si-B phase was formed during deposition is undetermined. Examination of Figure 27 tends to discount any phase formation for 20% SiO_2 /80% BN and highlights the improved across wafer tolerance obtained from 93% BN which has been

* sample broke from
scribing



0	-1	0	+2
*	-1	0	0
+1	0	0	*
*	0	+1	+1

93% BN



-10	*	-6	-1
-10	-8	-3	+1
*	0	+2	+3
+4	+6	+10	*

80% BN/20% SiO₂

Figure 27 - % Sheet Resistance Variation Across Silicon
Wafer for 93% BN and 80% BN/20% SiO₂

shown to form a Si-B phase. Observed across wafer tolerances for 20% SiO₂/80% BN are, respectively, $\pm 10\%$ and $\pm 1-2\%$.

In order to determine what effect the use of BN wafers with different densities and binder concentrations a test run was made with three runs of 40 silicon each using a randomly selected BN wafer. The results are shown in Figure 28 as a plot of frequency of sheet resistance for all 120 wafers processed and the data indicates that 95% of all sheet resistance measurements fell within ± 2.8 ohms/square of the 64 ohms/square norm ($\pm 4\%$ of norm). This indicates that even with non optimized conditions as far as BN wafer composition is concerned it is possible to achieve good results.

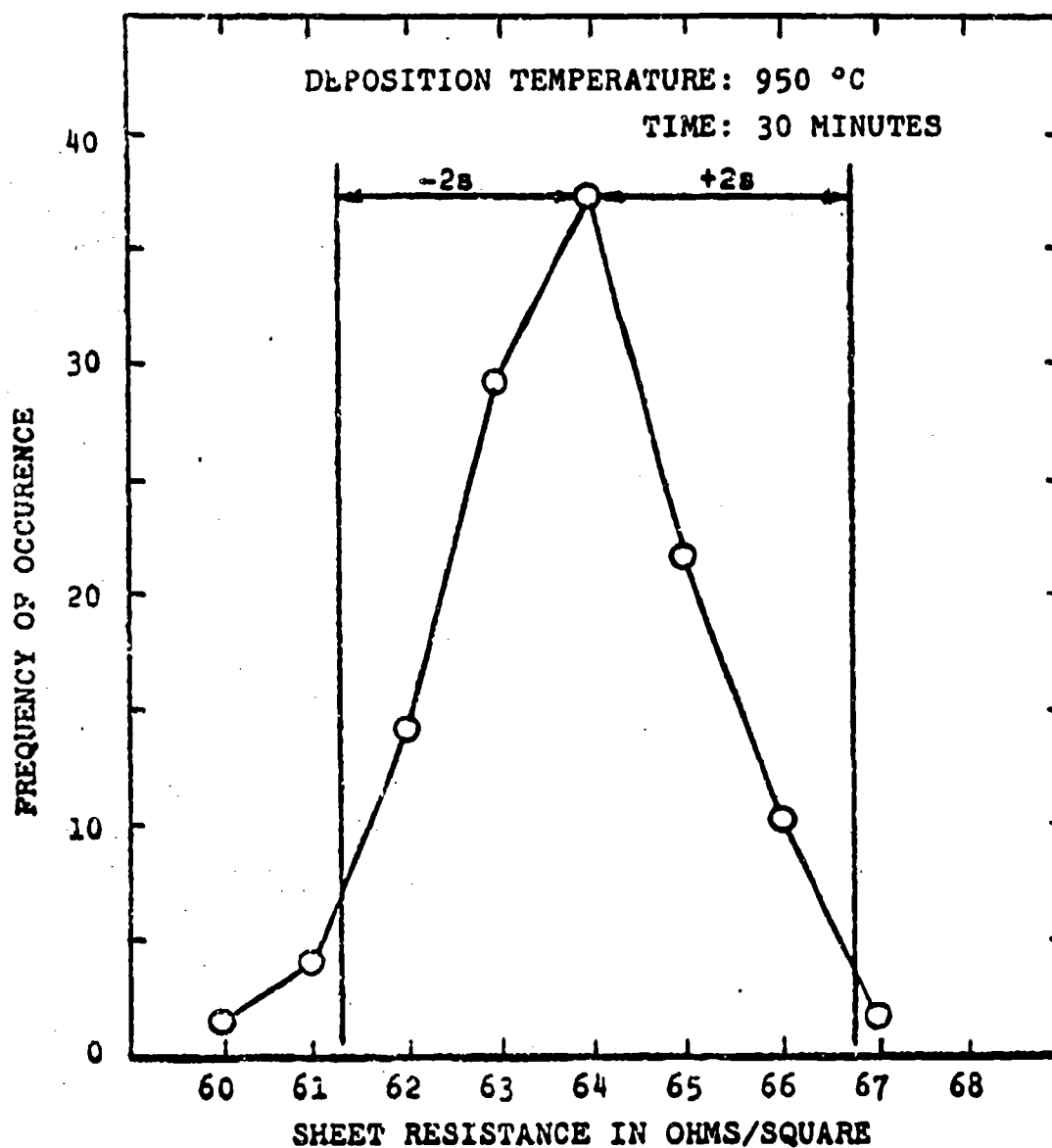


Figure 28 - Sheet Resistance Distribution

N TYPE SOURCE EVALUATION

During the terms of the investigation of BN wafer sources a preliminary study was made on the possibility of developing an N type planar wafer source. The goal was an arsenic source but only a phosphorus source was developed and tested during this phase of the investigation. Two N type sources were tested the most promising of which was a material developed by Owens-Illinois (30). The material is high purity aluminum metaphosphate (AMP) and SiO_2 . Tests were conducted for oxide formation, PSG penetration, sheet resistance and junction depth. Figures 29 and 30 show the data obtained. From these preliminary tests, it appears that AMP is a very attractive N type source and its high purity is also very attractive. Further studies are needed to determine additional process variables.

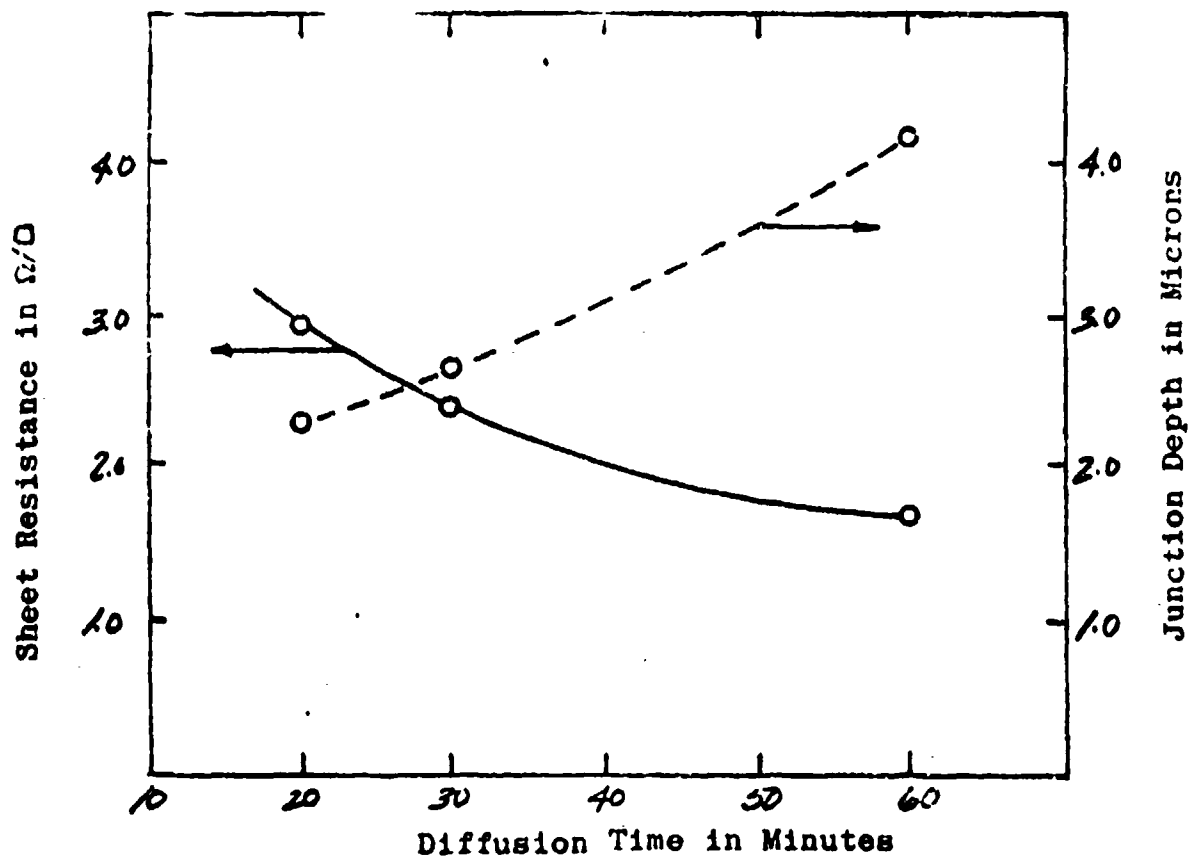


Figure 29 - Sheet Resistance, Junction Depth Versus Time - 1100°C

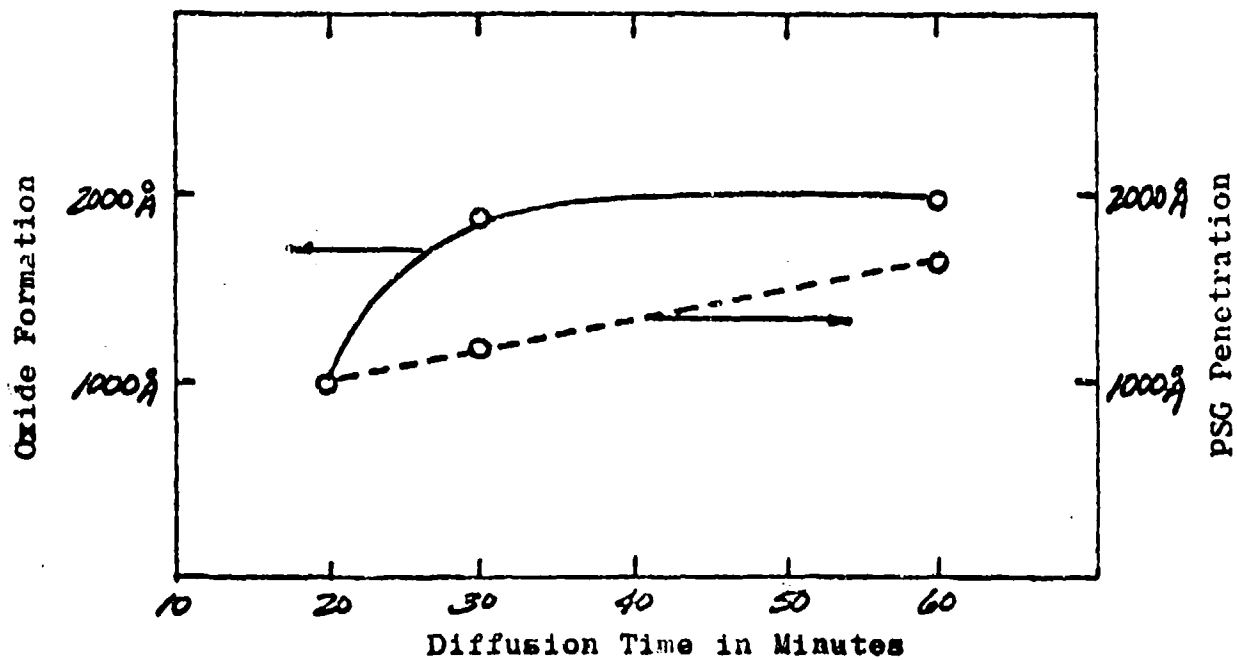


Figure 30 - Oxide Formation, PSG Penetration Versus Time, 1100°C

REFERENCES

5.

1. R. P. Donovan, Section I, Fundamentals of Silicon Integrated Device Tech., Volume I, 309, R. M. Burger and R. P. Donovan, Editors, Prentice-Hall (1967).
2. M. J. Rand and J. F. Roberts, "Preparation and Properties of Thin Film Boron Nitride," J. Electrochem. Soc., 115, 432 (1968).
3. Handbook of Chemistry and Physics, published by Chemical Rubber Company, 38, 430 (1956).
4. R. Speiser, S. Naiditch, and H. L. Johnston, "The Vapor Pressure of Inorganic Substances. $\text{H}_2\text{B}_2\text{O}_3$," J. Am. Chem. Soc., 72, 2578 (1950).
5. J. R. Soulen, P. Sthapitanonda, and J. L. Margrave, "Vaporization of Inorganic Substances; B_2O_3 , TeO_2 and Mg_3N_2 ," J. Phys. Chem., 59, 132 (1955).
6. S. P. Randall and J. L. Margrave, "Vapour Equilibria in the $\text{B}_2\text{O}_3\text{-H}_2\text{O}$ System at Elevated Temperatures," J. Inorg. Nucl. Chem., 16, 29 (1960).
7. M. C. Duffy, D. W. Foy, and W. J. Armstrong, "Diborane for Boron Diffusion in Silicon," Electrochemical Tech., 5, 29, (1967).
8. E. Milkova, "Gas Flow Influence on the Uniformity of Diffused Dopant Distribution in Silicon," S&T and Solid State Technology, no vol. no., 29 (1967).
9. K. Vedam, W. Knausenberger, and F. Lukes, "Ellipsometric Method for the Determination of All the Optical Parameters of the System of an Isotropic Nonabsorbing Film on an Isotropic Absorbing Substrate. Optical Constants of Silicon," J. Opt. Soc. Am., 59, 64 (1969).
10. K. Vedam and S. S. So, "Characterization of Reel Surfaces by Ellipsometry," Surface Science, 29, 379 (1972).
11. R. J. Archer, and G. W. Gobeli, "Measurement of Oxygen Adsorption on Silicon by Ellipsometry," J. Phys. Chem. Solids, 26, 343 (1965).
12. K. M. Busen, W. A. FitzGibbons, and W. K. Tsang, "Ellipsometric Investigations of Boron-Rich Layers on Silicon," J. Electrochem. Soc., 115, 291 (1968).
13. G. L. Vick and R. M. Whittle, "Solid Solubility and Diffusion Coefficients of Boron in Silicon," J. Electrochem. Soc. 116, 1142 (1960).

14. P. A. Miles and J. Holbenhan, "Diffusant Impurity-Concentration Profiles in Thin Layers on Silicon," Solid-State Electronics, 5, 331 (1962).
15. S. Maekawa and T. Oshida, "Diffusion of Boron into Silicon," J. Phys. Soc. Jap., 19, 253 (1964).
16. K. H. Nicholas, "Studies of Anomalous Diffusion of Impurities in Silicon," Solid-State Electronics, 9, 35 (1966).
17. T. J. Parker, "Diffusion in Silicon. I. Effect of Dislocation Motion on the Diffusion Coefficients of Boron and Phosphorous in Silicon," J. Applied Physics, 38, 3471 (1967).
18. N. D. Thai, "Anomalous Diffusion in Semiconductors - A Quantitative Analysis," Solid-State Electronics, 13, 165 (1970).
19. R. B. Bird, W. E. Stewart, and E. N. Lightfoot, Transport Phenomena, John Wiley and Sons, Inc., 510 (1960).
20. R. P. Donovan, "Alternative Method for Converting Incremental Sheet Resistivity Measurements into Profiles of Impurity Concentration," Solid-State Electronics, 10, 155 (N) (1967).
21. E. F. Duffek, E. A. Benjamini and C. Mylroie, "The Anodic Oxidation of Silicon in Ethylene Glycol Solutions," Electrochem. Tech., 3, 75 (1965).
22. F. Reizman and W. Van Gelder, "Optical Thickness Measurement of SiO_2 - Si_3N_4 Films on Silicon," Solid-State Electronics, 10, 625 (1967).
23. D. Gray, Private Communication.
24. E. Milkova, "Gas Flow Influence on the Uniformity of Diffused Dopant Distribution in Silicon," SCP and Solid State Technology, no vol. no., 29 (1967).
25. M. C. Duffy, D. W. Foy, and W. J. Armstrong, "Diborane Dopant Diffusion in Silicon," Electrochemical Tech., 5, 29 (1967).
26. W. J. Armstrong and M. C. Duffy, "A Closed-Tube Technique for Diffusing Impurities into Silicon," Electrochemical Technology, 4, 475 (1966).
27. S. P. Randall and J. L. Margrave, "Vapour Equilibria in the B_2O_3 - H_2O System at Elevated Temperatures," J. Inorg. Nucl. Chem., 16, 29 (1960).
28. T. Miles, Private Communication.
29. D. N. Gray and E. Smith, Owens-Illinois Technical Center, Toledo, Ohio.
30. W. R. Runyun, "Silicon Semiconductor Technology," McGraw-Hill (1965).